

**THE EFFECT OF SINTERING ADDITIVES ON
THE MECHANICAL PROPERTIES OF LIQUID
PHASE PRESSURE-LESS SINTERED ALUMINA**



By

Nasbah Bint Monir

School of Chemical and Materials Engineering (SCME)

National University of Sciences and Technology (NUST)

2022

THE EFFECT OF SINTERING ADDITIVES ON THE MECHANICAL PROPERTIES OF LIQUID PHASE PRESSURE-LESS SINTERED ALUMINA



Name: Nasbah Bint Monir

Registration number: 0000275215

This thesis is submitted as a partial fulfilment of the requirements

for the degree of

MS in Nanoscience and Engineering

Supervisor Name: Dr. Adeel Umer

School of Chemical and Materials Engineering (SCME)

National University of Sciences and Technology (NUST)

H-12 Islamabad, Pakistan

September, 2022

Thesis acceptance certificate

Certified that final copy of MS/MPhil thesis written by Ms **Nasbah Bint Monir**, (Registration No 0000275215), of School of Chemical and Materials Engineering (SCME) has been vetted by undersigned, found complete in all respects as per NUST Statutes/Regulations, is free of plagiarism, errors and mistakes and is accepted as partial fulfillment for award of MS degree. It is further certified that necessary amendments as pointed out by GEC members of the scholar have also been incorporated in the said thesis.

Signature: _____

Supervisor: **Dr. Malik Adeel Umer**

Date: _____

Signature (HOD): _____

Date: _____

Signature (Dean/Principal): _____

Date: _____

Dedication

I would like to dedicate the thesis work in the memory of my beloved mother who departed from this world last year, on 7th October,2021 and to my father, siblings, my husband, teachers and friends especially Mah Rukh Rehman and to the people in my life who always put up their trust and supported, guided and assisted me in the best and worst.

Acknowledgement

All praise to Allah Almighty - Lord of the Worlds, for His help and utmost support to the completion of this work.

My special gratitude for my supervisor and mentor Dr. Adeel Umer, whose trust, training, support and guidance were my motivation and of immense importance throughout. His endless support and guidance were the key to successful completion of this research work.

I would also like to extend my gratitude to the members of Guidance and Evaluation Committee Dr. Farhan, Dr. Zakir Hussain and Dr. Iftikhar H Gul for their endless support throughout the thesis project.

I would also like to pay gratitude to the supporting staff of SCME for their assistance during the research.

Last, but not the least, all my success and achievement would not have been possible without the extreme care, support, prayers and love of my parents and my siblings. Their assistance and encouragement have always been the ultimate source of success for me.

Nasbah Bint Monir

Reg 0000275215

Abstract

Al_2O_3 is one of the most used ceramic oxides that finds a lot of structural applications. The thesis explores a low temperature sintering route of alumina through the addition of sintering additives that employ a hybrid liquid and solid-state sintering enhancements that can potentially promote sintering at relatively low temperatures. The sintering additives used are primarily mixtures of CuO and TiO_2 in different combinations. The basis of study was made initially on the interaction of alumina with CuO, added in amount of 1wt%, 3wt%, 5wt% and 8wt%. Afterwards the study of addition of TiO_2 was observed in the Al_2O_3 - CuO system mentioned earlier. It was observed that the densification of Al_2O_3 improved upon the addition of these two aids, in comparison to pure alumina sintered at same temperature(s). The mechanical properties of the sintered pellets were also studied for both the systems and a comparative study was established. It was revealed that the hardness increased by the addition of TiO_2 in Al_2O_3 -CuO system. The best results for mechanical properties were obtained for the samples containing a 5wt% of copper oxide. CuO enhanced densification via the formation of a liquid phase at alumina-alumina grain boundaries which enhanced densification kinetics, while the addition of TiO_2 creates vacancies in the Al_2O_3 lattice which promotes solid state sintering. A combination of these two phenomena is expected to promote sintering and densification at relatively lower temperatures, used for sinter alumina conventionally. Upon the addition of the two, densification increased leading to an increase in micro-vickers hardness values from 17.5 GPa to 31.5 GPa at 1300 °C, and from 21.38GPa to 45.66 GPa at 1400 °C. While the compression at 1300 °C of Al_2O_3 - CuO system was 2.284 GPa while upon the addition of TiO_2 its value increased to 6.29 GPa. At 1400 °C the value increased from 4.003GPa to 8.34GPa. Further, in alumina multiphase system CuO- TiO_2 - ZrO_2 were added and studied. The optimized concentration i.e 5wt% CuO- TiO_2 , was considered and ZrO_2 (1wt% and 5wt%) was added. The results showed drastic decrease in the densification and mechanical properties of alumina.

Table of Contents

CHAPTER 1	1
1. INTRODUCTION	1
1.1. Ceramics	1
1.1. Ceramic Structure	2
1.1. Types of ceramics	4
1.3.1. Traditional Ceramics	5
1.3.2. Advanced Ceramics	5
1.3.2.1. Crystalline Ceramics	5
1.3.2.2. Non-crystalline Ceramics	6
1.4. Three Distinct Categories of Ceramics	6
1.4.1. Oxides	6
1.4.2. Non-Oxides	7
1.4.3. Composites	7
1.5. Properties	8
1.5.1. Density	9
1.5.2. Mechanical Properties	9
1.5.2.1. Hardness	10
1.5.2.2. Compression Testing	12
1.5.3. Fractography	15
1.5.4. Thermal Properties	17
1.6. Motivation	18
1.7. Objectives	19
CHAPTER 2	20
2. LITERATURE REVIEW	20
2.1. Alumina	20

2.2. Structure of Alumina	19
2.3. α - Alumina	21
2.4. Ceramography	22
2.5. Sintering	23
2.5.1. Solid state sintering	24
2.5.2. Liquid phase sintering	24
2.5.2.1. Wetting	26
2.5.2.3. Dihedral angle	27
2.5.2.3. Solid solubility in liquid	28
2.6. Stages of liquid phase sintering	29
2.6.1. Particle rearrangement	29
2.6.2. Solution-reprecipitation	30
2.6.3. Solid-state controlled sintering	30
2.7. Sintering Additives	31
2.7.1. Material choice as sintering additives	34
2.7.1.1. Copper oxide (CuO).....	34
2.7.1.2. Titania (TiO ₂)	36
2.7.1.3. Zirconia (ZrO ₂)	38
CHAPTER 3	42
3. EXPERIMENT AND CHARACTERIZATION	42
3.1. Experimental route	42
3.2. Sample Preparation	42
3.2.1. Synthesis of Copper oxide	42
3.2.2. Material preparation and sintering	43
3.2.2.1. Alumina: Copper oxide	43
3.2.2.2. Alumina: Copper oxide: Titania	45
3.2.2.3. Alumina: Copper oxide: Titania: Zirconia	45
3.2.3. Mounting	46
3.2.4. Grinding.....	46
3.2.5. Polishing.....	46

3.3. Characterization techniques	47
3.3.1. X-ray diffraction (XRD)	47
3.3.2. Scanning Electron Microscope (SEM)	49
3.3.3. Density measurement	50
3.3.4. Micro- Vickers Hardness	51
3.3.5. Universal Testing Machine (Shamizdu AG-X plus) (UTS)	53
CHAPTER 4	55
4. RESULTS AND DISCUSSION	55
4.1. XRD	55
4.2. Scanning Electron Microscopy	58
4.3. Density Measurement.....	64
4.4. Micro-Vickers Hardness	70
4.5. Universal Testing Machine	74
Chapter 5 Conclusion	80
References	82

List of Figures

Figure 1 Historical timeline of the development of materials	2
Figure 2 Anions surrounded by cations.....	3
Figure 3 General schematics of ceramic in general.....	4
Figure 4 Schematics of Vickers Hardness test	11
Figure 5 Demonstration of force applied during bend test (A)Spring test (B) bend test.....	13
Figure 6 Assembly of the sample during compression testing.....	14
Figure 7 Flexural test schematics.....	17
Figure 8 Structure of Alpha alumina, the grey spherical represents aluminium ion while black dots represent oxygen ions	21
Figure 9 Represents the sintering stages.....	23
Figure 10 Different stages of liquid phase sintering.....	25
Figure 11 Wetting on the solid surface.....	26
Figure 12 Complete penetration of liquid when dihedral angle is 0°	27
Figure 13 Schematics of change in densification wrt sintering time.....	31
Figure 14 Phase diagram of alumina and copper oxide.....	35
Figure 15 Titania (Rutile) unit cell, where black dot represents Oxygen and Ti is represented by white dots.....	36
Figure 16 Phase diagram of Alumina- Titania system.....	37
Figure 17 Diagram presenting layout of experimental work.....	40
Figure 18 Powder form α -Al ₂ O ₃	41

Figure 19 Temperature vs time graph of sintering.....	42
Figure 20 Represents the general schematics of the experimental work	44
Figure 21 Diffraction of light beam demonstration.....	47
Figure 22 Schematics of sample interaction during SEM.....	48
Figure 23 Densification measurement apparatus.....	49
Figure 24 Schematics of indent in Vickers hardness apparatus.....	50
Figure 25 Graph representing stress/ strain curve during compression.....	52
Figure 26 XRD comparison of Al ₂ O ₃ and Al ₂ O ₃ -CuO.....	53
Figure 27 XRD comparison of Al ₂ O ₃ and Al ₂ O ₃ -CuO-TiO ₂	54
Figure 28 XRD comparison of Al ₂ O ₃ -CuO-TiO ₂ and Al ₂ O ₃ -CuO-TiO ₂ -ZrO ₂	55
Figure 29 SEM image of pure alumina at (a) 1300°C, (b) 1400°C.....	56
Figure 30 SEM images of at 1300C (a) Al ₂ O ₃ - 1wt% CuO, (b) Al ₂ O ₃ - 3wt% CuO, (c) Al ₂ O ₃ - 5wt% CuO, and (d) Al ₂ O ₃ - 8wt% CuO.....	57
Figure 31 SEM image of 5wt% CuO at 1400C and EDS.....	58
Figure 32 SEM image of Al ₂ O ₃ -5wt% CuO-TiO ₂ at a)1300°C and b) 1400°C.....	59
Figure 33 SEM images of a) Al ₂ O ₃ -CuO-TiO ₂ -1 wt%ZrO ₂ and b)Al ₂ O ₃ -CuO-TiO ₂ -5wt%ZrO ₂ at 1300 °C	61
Figure 34 SEM images of a) sAl ₂ O ₃ -CuO-TiO ₂ -1 wt%ZrO ₂ and b)Al ₂ O ₃ -CuO-TiO ₂ -ZrO ₂ at 1400°C	62
Figure 35 Relative density graph of pure alumina and Al ₂ O ₃ -CuO system at (a)1300°C and (b)1400°C	64
Figure 36 Comparison of Relative density graph of pure alumina and Al ₂ O ₃ -CuO system at (a)1300°C and (b)1400°C	64

Figure 37 Relative density graph of pure alumina and Al ₂ O ₃ -CuO- TiO ₂ system at (a)1300°C and (b)1400°C	65
Figure 38 Relative density graph of pure alumina and Al ₂ O ₃ -CuO-TiO ₂ system at (a)1300°C and (b)1400°C	66
Figure 39 Relative density comparison of Al ₂ O ₃ -CuO and Al ₂ O ₃ -CuO-TiO ₂ system.....	67
Figure 40 Density comparison of Al ₂ O ₃ -CuO-TiO ₂ and Al ₂ O ₃ -CuO-TiO ₂ - (1,5 wt%) ZrO ₂	68
Figure 41 Vickers Hardness of pure alumina and Al ₂ O ₃ -CuO system at (a)1300°C and (b)1400°C.....	69
Figure 42 Vickers Hardness graph of pure alumina and Al ₂ O ₃ -CuO- TiO ₂ system at (a)1300°C and (b)1400°C	70
Figure 43 Vickers Hardness values of (a) Al ₂ O ₃ -CuO and (b) Al ₂ O ₃ -CuO-TiO ₂ at 1300°C and 1400°C	71
Figure 44 Vickers Hardness values comparative study of Al ₂ O ₃ -CuO and Al ₂ O ₃ -CuO-TiO ₂	72
Figure 45 Vickers Hardness values comparison of Al ₂ O ₃ -CuO-TiO ₂ and Al ₂ O ₃ -CuO-TiO ₂ -(1-5 wt%) ZrO ₂	73
Figure 46 Vickers Hardness values comparison of Al ₂ O ₃ -CuO-TiO ₂ and Al ₂ O ₃ -CuO-TiO ₂ -(1-5 wt%) ZrO ₂	74
Figure 47 Compression testing graph of pure alumina and Al ₂ O ₃ -CuO-TiO ₂ system at (a)1300°C and (b)1400°C	75
Figure 48 Compression testing graph of (a) Al ₂ O ₃ -CuO and (b) Al ₂ O ₃ -CuO-TiO ₂ at 1300°C and 1400°C	76
Figure 49 Comparative study of ompression testing values of (a)Al ₂ O ₃ -CuO and (b)Al ₂ O ₃ -CuO-TiO ₂	77
Figure 50 Compression testing values comparison of Al ₂ O ₃ -CuO-TiO ₂ and Al ₂ O ₃ -CuO-TiO ₂ - (1-5 wt%) ZrO ₂	78

Figure 51 Represents values of 5wt% CuO added in $\text{Al}_2\text{O}_3\text{-CuO}$ and $\text{Al}_2\text{O}_3\text{-CuO-TiO}_2$ system at 1400°C79

List of Tables

Table 1 Represents condition for homogenous mixing of powdered samples.....	41
Table 2 Composition of Alumina system addition of Copper oxide.....	42
Table 3 Composition of Alumina system addition of Copper oxide- Titania.....	43
Table 4 Composition of Alumina system addition of Copper oxide-Titania-Zirconia.....	44
Table 5 EDS weight ratio focused on specific area.....	58
Table 6 EDS weight ratio focused on specific area	59
Table 7 EDS weight ratio focused on specific area	61
Table 8 EDS weight ratio focused on specific area.....	63

Chapter 1

Introduction

In the modern world it is a widely accepted paradigm that development and technological progress, which is taking place, in a highly competitive environment in various fields, provides pathways to overcome the exhaustion of the limited resources, thus helping mankind to meet its needs as hunger over the raw material has been a driving force.

Alumina one of the naturally occurring compound found in earth's crust as corundum, an amorphous substance that can react with both acids and bases. Alumina known as aluminum oxide or aloxide has been used for centuries in the form of clay and in various ceramic products.

Alumina due to its outstanding properties, has contributed to a significant number of life-extending and society-enhancing applications. As alumina is widely being used for structural applications, including for armor that can defeat high-velocity projectiles with various cores, used in wear resistance applications and in applications where mechanical strengths are coupled with corrosive and thermal actions.-(Medvedovski, 2006)

1.1.Ceramics

To understand the importance of alumina it is necessary to grasp the understanding of the ceramics in general. A ceramic is a naturally occurring inorganic raw material which includes oxides, carbides, nitrides, sulfides, and fluorides. A ceramic sensu-strictu is an oldest man-made material, which is made by shaping and firing a nonmetallic mineral, such as clay, at a very high temperature. Common examples are earthenware, porcelain, and brick. These materials are at least 30% crystalline in nature. These materials are shaped at ambient temperatures by large variety of forming techniques (Medvedovski, 2006) (Heimann, 2010).

Ceramic materials are the most versatile branch of materials. They possess excellent mechanical properties under extreme conditions of tension; high hardness, heat-resistant and corrosion-resistant

inorganic materials constituted by the combination of metallic and nonmetallic elements, magnetic or optical properties, showing resistance to chemical and corrosive environments. (Medvedovski, 2006), (C, 1991) . These attributes mentioned allow ceramics to be used for a large number of applications i.e from household materials such as bricks blocks, tiles, floors, along with industrial applications such as refractories, fillers, cutting tools, coating reactors, nuclear ceramics etc (C, 1991).

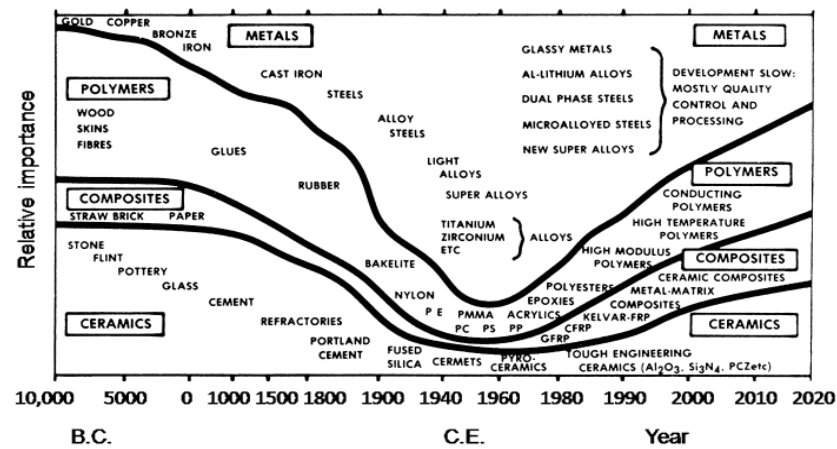


Fig. 1. Historical timeline of the development of materials (Medvedovski, 2006)

In early centuries ceramics have been vastly used till 155C.E. after which metal technology took over. However, in 1970's decline was seen when application of emerging polymers played a very important role, thus decreasing impact of metal usage. Today plastic engineering has even more impacted a decline in the usage of metals (L.L, 1988). The field of ceramic research has dominated for the last 40 years by work on technical ceramics.

1.2.Ceramic Structure

The crystallinity of ceramic materials ranges from highly oriented to semi-crystalline, vitrified or completely amorphous. The property of a ceramic depends on the nature and directionality of the interatomic bonds and the atomic packing of these materials causing versatility. These materials are

mainly constituted by strong ionic and covalent bonds i.e. primary bonds, hydrogen bonds and van der Waals forces i.e. secondary bonds, in different proportions. These bonds determine a series of specific properties of ceramic materials among which are relatively high fusion temperatures, high modulus, high wear strength, durability, poor thermal properties, high hardness and fragilities combined with tenacities, and low ductility. (Subedi, 2013)

The type of bonding occurs in ceramic material are ionic bond and covalent bond. These bonds define the characteristic of a ceramics as sometime these bonds co-exist with in a same ceramic material. The ionic bonds usually occur between metallic and non-metallic elements. These have large differences in electronegativities, due to which strong bond is formed. This increases the melting point of such ceramics, since they are non-directional. (L.L, 1988) (Subedi, 2013). The covalent bond occurs in ceramic is where electrons are transferred, atoms bonded equally share the electrons, thus forming a stabilized structure. (Subedi, 2013)

Ceramic crystal structures constitute of anions surrounding a cation and are all in contact with it. This leads to lack of conduction electrons since they are combined forming chemical bonds. For a specific coordination number there is a critical or minimum cation-anion radius ratio r_C/r_A for which this contact can be maintained. There is a large range of possible options for the composition and structure formation of a ceramic, this plays an important role for identifiable attributes in ceramics i.e. hardness, toughness, and good electrical and thermal insulators. (C, 1991)

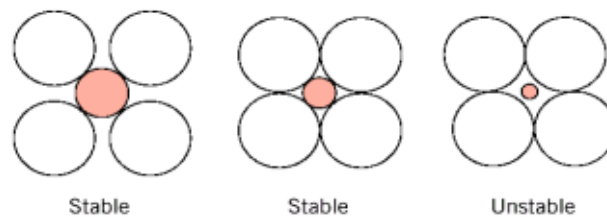


Fig 2. Anions surrounded by cations

These attributes further depend on the ceramic's microstructure i.e its either amorphous, crystalline, or polycrystalline solids. These structures contain number of single crystals that are separated by areas of disorder known as grain boundaries. Grain boundary is a planar defect with same composition but

different orientation. These grains range from $1\mu\text{m}$ to $50\mu\text{m}$. Thus, the ceramics can be defined as microstructure dependents, constitute of grains, porosity, second phases etc. (Kingery W. , 1976)

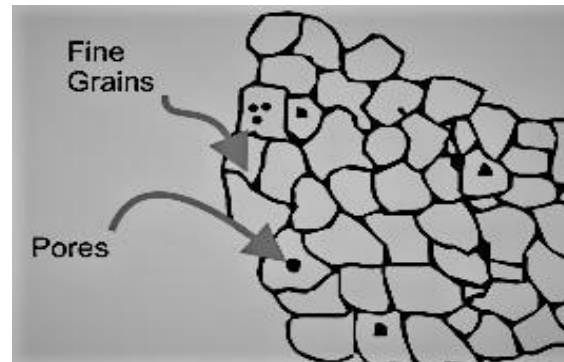


Fig 3. General schematic of ceramic in general

1.3.Types of Ceramics

Ceramic materials have been defined in material science as inorganic, non-metallic, often crystalline oxide, nitride, or carbide material. Some elements, such as carbon or silicon, may be considered ceramics.

Ceramic materials can be divided into two large groups:

1. Traditional ceramics
2. Advanced ceramics.
 - 2.1. Crystalline Ceramics
 - 2.2. Non-Crystalline Ceramics

1.5.1. Traditional Ceramics:

Generally, the ceramic powders extracted directly from minerals are going to be used in traditional ceramics, which are high-volume materials. The starting material for traditional ceramics is in raw state obtained from natural deposits such as clay material, having impurities, this raw material need to

undergo processes for the elimination of impurities and the obtained material should be such that it can be subjected to the reproducible method in order to obtain a powder that can be shaped and sintered to obtain a piece. These can be defined as those that are based on silicates, among which are cement, clay products, and refractories. The benefit of these traditional ceramics is that they can be produced in large volumes and thus constitute a dominant market. (Kingery W. , 1976)

1.5.1. Advanced Ceramics:

The advanced materials are considered to be special, engineered, or technical ceramics. For the last 100 years work on these materials has been in progress. The particulate systems obtained by a more advanced and sophisticated synthetic route help in achieving artificial raw material with high purity. These ceramics have greater application in the modern world, which implies that the control of impurities and defects is more important in the final application.

The powders produced synthetically by opting various routes have common characteristics, such as high purity, great uniformity as uniform particle size distribution is achieved with no hard aggregates or agglomeration and high specific surface area throughout the sample. The treated ceramics includes carbides, nitrides, borides, pure oxides, and a great variety of ceramics with magnetic, ferroelectric, piezoelectric, and superconducting applications, etc. The properties of these ceramics is also enhanced as they possess excellent mechanical properties under tension, high wear strength or excellent electrical, magnetic, or optical properties, or exceptional strength to high temperatures and corrosive environments, showing high strength to chemical attack. (Heimann, 2010) (Kingery W. , 1976)

1.5.1.1. Crystalline Ceramics

Crystalline ceramic materials have a lattice point which is occupied by atom or ion, this depends on the bonding mechanism. The arrangement of atoms or ions is regular, forming three-dimensional structure. Due to this these ceramics are not amenable to a great range of processing. Specific methods are considered when dealing with these materials, which usually are shaping, slip casting, tape casting, mold injection, dry pressing etc.

In most cases these materials tend to fall into a category of "Forming" powders into the desired shape, and then sintering to form a solid body.

1.5.1.2. Non-crystalline Ceramics

Non-crystalline ceramics are amorphous in nature exhibiting short range order or pattern of atoms or ions. The density lies intermediate in between polymers and metals thus, these are less dense than crystalline ceramic materials. Normally glass lies in the nanocrystalline ceramic category. These tend to be formed from melts and are shaped when either fully molten, by casting, or when in a state of viscosity, by methods such as blowing into a mold. Glass ceramics can be formed that is, having short range order thus making it partially crystalline. This can be used in various applications as cook-tops or for nuclear waste disposal. (Subedi, 2013)

1.4. Three Distinct Categories of Ceramics

Ceramics can also be classified into material categories:

1.4.1. Oxides:

These materials consists of inorganic compounds of metallic or metalloids such as alumina, titanium, zirconia, magnesium, silicon with oxygen. These have enhanced mechanical properties thus used in various applications. The metal being in its oxide state is the most stable material which is favorable in harsh oxygen containing conditions such as in industrial processes and application environment. Yet oxide ceramics are not always well-suited especially in extreme environments or in applications which require bearing significant load. (SadatMirdamadi, 2021)

1.4.2. Non-oxides:

Oxide ceramics are not always well-suited especially in extreme environments or in applications which require bearing significant load. Due to this there is a need of even more stable ceramics required to withstand such harsh conditions, non-oxide respond to this need. These materials are covalent bonded ceramics. Due to the covalent bond which leads to low atomic diffusivity thus, make these materials difficult to sinter conventionally. These materials have high thermal conductivity and low thermal expansion coefficient. (SadatMirdamadi, 2021)

1.4.3. Composites:

A composite material composed of two or more constituent materials, having different physical and chemical properties. The components remain distinct within finished structures These materials where ceramics are used as reinforcement and as a matrix are special type of composite materials. The ceramic composite materials exhibiting quasi-ductile fracture behavior. Due to high processing temperature, fibers that are stable above 800°C to 1000°C can only be used e.g. zirconia or alumina etc., Within these ceramics various combinations of oxides and non-oxides are also included. Their applications are in fields requiring resistance to corrosion and wear and reliability at high temperatures. In various fields the ceramics composite properties can be utilized such as in heat shield systems, flame holders, brake system components etc. (FatimaZivic, 2021)

As these materials are being utilized in applications as hardness and strength is improved, but when it comes to the brittle nature of ceramics even in ceramic composites, this cannot be ignored especially when subjected to prolonged exposure of load and stresses thus degradation and damage occurs to these materials. This can be explained when manufactured at high processing temperature, giving complexity in manufacturing process as difference in thermal expansions within compacts causes high level porosity and cracks propagation occurs in them.

1.5. Properties

Ceramics substance physical properties are a direct result of its crystalline structure and chemical composition. Thus, these materials can withstand harsh surroundings such as chemical erosion that occurs in other materials subjected to acidic environments. In structure due to the arrangement of atoms in a most stable state ceramics generally can withstand very high temperatures, ranging from 1,000 °C to 1,800 °C.

Solid-state chemistry reveals the understanding of ceramic structure explaining fundamental connection between microstructure and properties, such as localized density variations, grain size distribution, type of porosity, and second-phase content, which can all be correlated with ceramic properties such that is mechanical properties (**Hall-Petch equation**), like hardness, toughness, dielectric constant, and the optical properties exhibited by transparent materials.

Ceramic material lack in elasticity, one of the prominent limitations of these materials in structural applications is the fragility, upon any absorption of energy they tend to fracture in a fragile way, as they lack capacity for plastic deformation, especially under friction or drag. This fragility to the fracture can be explained to a great extent, the presence of strong covalent forces and due to the presence of defects in the material these intensifies the resistant to compressive forces than to tension forces. As a result, this behavior makes it difficult to eliminate or hinders the movement of the dislocations in ceramic structures, even at high temperatures. (RainerTelle, 2014) (B, 2009)

However, these structural ceramics have gained importance as it is being widely used to enhance and improve the mechanical properties. These uses require materials with high strength in various environmental conditions, capable of withstanding high temperatures and resistant to corrosion and oxidation. Also, these ceramic materials offer a substantial reduction in weight compared to other materials such as metals.

Some of the physical attributes of bulk ceramics include the following:

1.5.1. Density

1.5.2. Mechanical Properties

1.5.3. Thermal Properties

These properties are the intrinsic properties of the material, as small piece of the material has the same values as a large one. Mechanical properties of the material are scale independent in nature. This helps in simplifying the analysis of the structure. This is known as basic assumption of continuum mechanics. This is applicable on macroscale but as the size reduced to nano this assumption cannot be considered universal. (Pelleg, 2014)

1.5.1. Density

Density of a material describes the relationship of mass and the volume of the material. In general, is defined as mass per unit volume.

Mathematical representation,

$$\rho = \frac{m}{v}$$

where, ρ represents density, m represents the mass and v represents volume of the substance.

S.I. unit of density is kilogram per meter cubic i.e. kg/m³ and in cgs it is gram per cubic centimeter i.e. g/cm³

Density of a material depends on the change in microstructure when subjected to some external pressure and temperature. The pressure applied can be done using gas pressure, hot pressing, hot isostatic pressing. Also, density of a material depends on the additives added to increase its density. This promotes uniform size distribution once subjected to palletization and sintering, thus increasing density throughout the material. Densification is a process that includes pellets formation and briquetting. This helps to transform loosely packed material into a uniformly smooth surface material. (Fahrenholtz, 2004)

1.5.2. Mechanical Properties

Mechanical properties of a material determine a material behavior when subjected to stresses. The properties usually included elastic modulus, hardness, ductility, sor measure of strength. These defining properties of the material are mostly used in applications that improved in structural

applications which involves space and automobile industries. The material in a certain application is subjected to various mechanical forces and loads. The effect of these defines the nature or behavior of the material in a certain condition. Thus, the data determined by testing materials various mechanical properties provide insight on the material and its utilization in certain application. These properties also depend on the process of manufacturing of the material i.e. mold technique, pressure and temperature etc.

In modern materials science, the physics of stress and strain, strength, plasticity, stiffness, elasticity, brittleness, toughness, ductility fatigue, creep can help us understand the properties of the material in a detailed form. This helps in predicting the credibility of the material for its mechanical failure under the given circumstances. (Mordfin, 1968)

1.5.2.1. Hardness

Hardness is the measure of the material to resist deformation when various external loads are applied i.e. Mechanical indentation or aberration. The behavior of a solid material under force is complex. the resistance is related to the chemical bonds present in the material. Hardness can be measured by different techniques i.e. scratch hardness, indentation hardness and rebound hardness. Hardness of the material is dependent on plasticity strain strength toughness ductility and elastic stiffness. The common hard materials are ceramics metals concrete etc. Hardness is of critical significance to aggressive and erosive wear as it refers to the property of a material to resist pressing in or scratch off a sharp object. Hardness provides a qualitative relationship to other material properties under certain load. is not a fundamental property but has a range in which a certain material lies. The value of depends on the temperature structure and geometry of the material. (Ullner, 2001)

In ceramics is frequently a measured property, this helps to characterize resistance the fracture or deformation caused when in contact with other material.

Scratch hardness resistance of a sample to fracture or plastic deformation due to friction. It is used when testing coatings as the principal of it is that a hard material will scratch an object made of soft material

Indentation hardness measures the resistance of a sample to permanent deformation as it is subjected to a compression load from a sharp object. The hardness is characterized by the indentation formed in the material using a hard indenter. The indenter varies in shape and nature thus there are various machines to measure hardness such as Vickers, Knoop, Brinell and Rockwell. The commonly used machine for hardness testing is Vickers (Ullner, 2001). It has a pyramidal shaped diamond indenter with square base. The indentation area on the material depends on the shape of the indenter, loading force and rate, indentation size, time, surface condition and sample orientation. Using different loads can cause microcracking and deformation of indentation caused by the indenter. Materials that have a hardness larger than 40 GPa are considered to be super hard materials. Usually the average value of hardness of a material is considered to avoid ambiguity as defects present in the material can cause change in values (Ghorbal, 2017).

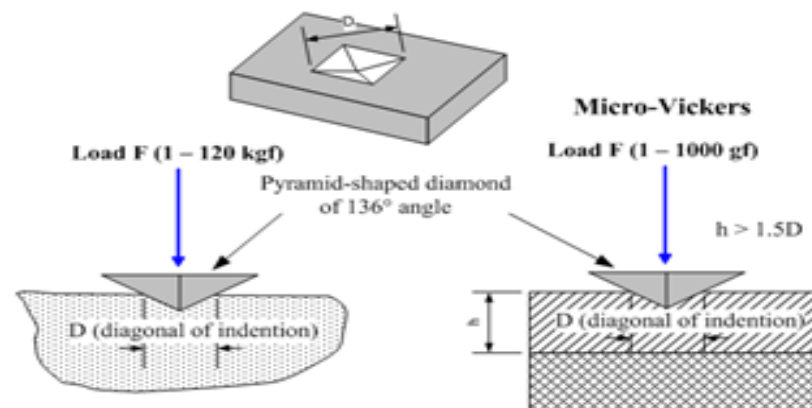


Fig 4. Schematics of Vickers Hardness test

Rebound hardness measures the height of the bounce of a diamond-tipped hammer dropped from a fixed height on to the material. The rebound hardness is also known as dynamic hardness. In this the velocity of an impact body before and after the impact is measured. This method is reliable than bench hardness testers.

Mathematically

$$HL = \frac{v_r}{v_i} \times 1000$$

Where v_r is the rebound velocity and v_i is the impact velocity.

1.5.2.2. Compression Testing

The ability of the material to resist any external crushing force applied without breaking or yielding by measuring fundamental variables such as strain, stress, and deformation. The testing machine involves load that squeezes the ends of a cylinder specimen between two plates. The process is notoriously difficult as repeated values can vary thus an average value is usually obtained. (Swab J. J., 2021)

During compressive loading, the relationship established between stress and strain is similar to that obtained during tensile loading. The trend is observed when material behaves elastically upon a certain value of stress applied, this means that stress is in proportion to strain. The ratio of height to diameter of the sample is set in a way so that buckling action can be avoided. Buckling action is a flexural torsional effect on the material when compression is applied i.e. the bending and twisting response of the material when subjected to an external load. (Sines, 2013)

Compression testing of material shows initially a linear relationship between stress and strain. This is the manifestation of Hooke's law

Mathematical representation

$$E = \text{stress/strain}$$

Where E is known as young's modulus for compression.

Strain in compression is defined as

$$e = \frac{h-h_0}{h_0}$$

Since height is reduced during compression, the value of e is negative which is ignored when expressing compression strain.

The value obtained exhibits the characteristic of the material to deform when a compressive load is applied before plastic deformation occurs. In the case of ceramics materials once plastic deformation occurs the material is likely to break as it has no elasticity. The permanent deformation of the material is the threshold known as the proportional limit. The force at which material reached its proportional limit is known as yield point or yield strength. The point where material breaks or is distorted gives ultimate compressive strength. In the case of ceramics fracture produced gives ultimate compressive strength value. (Sines, 2013)

The methods for the determination of compressive strength include flexural/bend test, spring test, or top load crushing.

The flexural bend test is used to determine the measure of the force required to bend a material, it determines the stiffness of the material. This test is also known as the three-point bending test, which is performed using the universal tensile testing machine. The results obtained by this method have some drawbacks as the method is sensitive to specimen and loading geometry and strain rate.

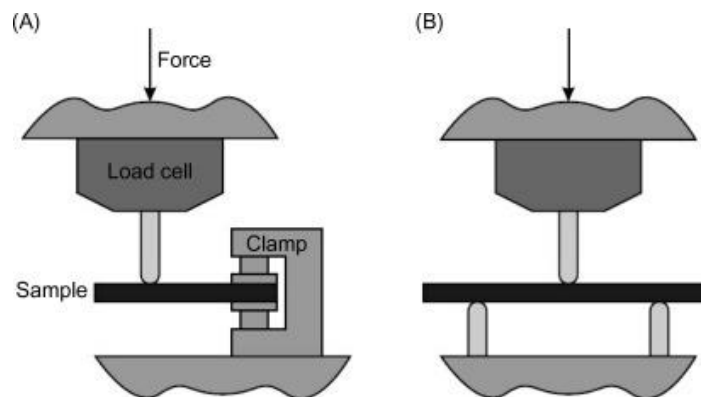


Fig 5. Demonstration of force applied during bend test (A)Spring test (B) bend test

Spring testing is specifically used for the springs which are the tightly wound coils shaped spiral of metal. Force is applied by pulling the subject outward that is stretching of the material takes place, but it returns to its initial state when this force is removed. It is highly used in the automobile industry (Swab J. J., 2019).

Top load crushing is a method when inward force is applied from the opposite sides of the material, which results into compressed, crushed or flattened. There are different types of compression testing i.e. uniaxial, biaxial, triaxial, cold temperature, elevated temperature, fatigue, or creep. The test sample is generally placed between the two plates this distributes the applied load across the entire surface area. Once the force is applied the plates are pushed together by a universal test machine. The compressed sample is short and in the direction of the applied forces and expands in the direction perpendicular to the force. the material is essentially crushed until failure.

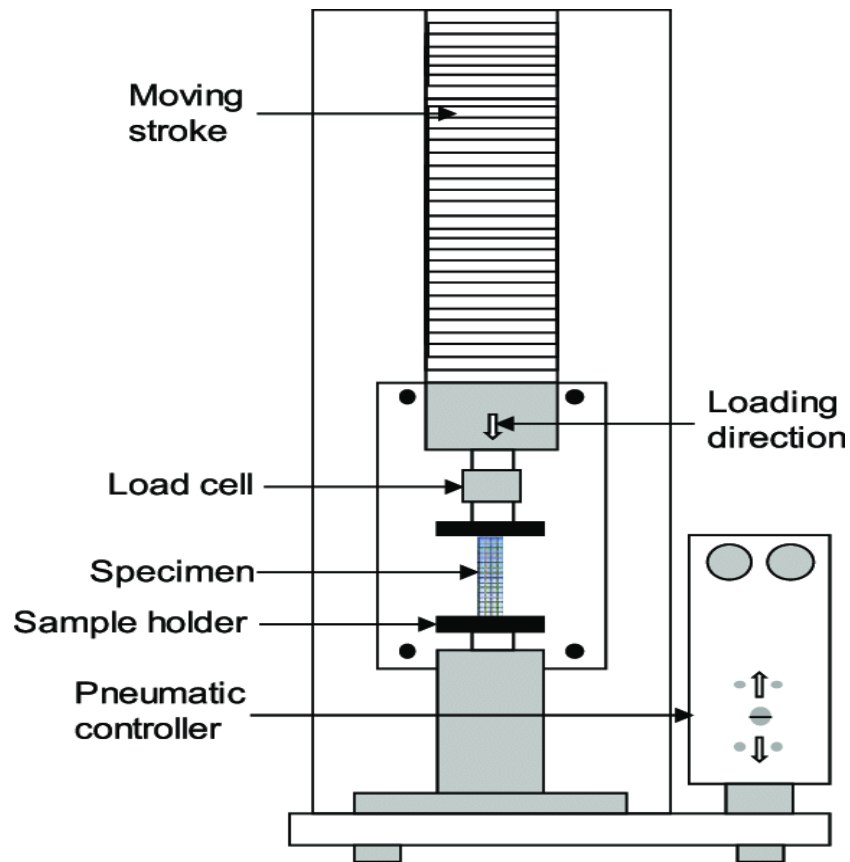


Fig 6. Assembly of the sample during compression testing

1.5.2.3. Fractography

Fractography also known as fracture toughness, is a process to measure the failure of the material by fracture mechanics. It is widely used to understand the causes of failures and verify the theoretical failure predictions with real-life failures.

Ceramic materials has ionic or covalent bonds, thus these are either crystalline or amorphous in nature. These materials has poor toughness as these are held together by either type of bond will tend to fracture before any plastic deformation takes place. The structure of the ceramic material is porous in nature, the pores and other defects acting as stress concentrators results in further decrease in toughness and reduction of tensile strength. (Möser, 1978)

However these materials do show plastic deformation as there are very few available slip systems for dislocations to move, and so they deform very slowly.

To overcome the brittle behavior, ceramic material development has introduced the class of ceramic matrix composite materials, in which Reinforcements are embedded forming fiber bridges or a medium across any crack. The purpose of it is to increase the fracture toughness of ceramics.

Toughness Is the quality of the material to absorb energy and plastically deform without fracturing. Toughness is given as the area under the stress strain curve. This means that toughness of the material can also be defined as the materials resistance to fracture when stress is applied. Ceramics are brittle in nature Thus these materials are strong but not tough the strength of the material defines nature of toughness of that material. To enhance the toughness of the material certain factors are important to consider such as the sintering temperature and duration, addition of additives which influence the microstructural morphology during the process, the cooling time etc.

Toughness can be determined by integrating the stress strain curve as it is defined as the mechanical deformation per unit volume before material is fractured mathematically

$$\frac{\text{energy}}{\text{volume}} = \int_0^{\epsilon_f} \sigma d\epsilon$$

Where e is strain

E_f is strain upon failure

σ is stress

There are several variables that have influence on the toughness of a material these variables are

Strain rate

Temperature

Notch effect

Since the material properties are not flawless and thus cannot be avoided during processing and fabrication which means material has a pre-existing flaw. Thus, fracture toughness is calculated which indicates the amount of stress required to propagate a pre-existing flaw. Flaws may appear as cracks, voids, defects or inclusions. Fracture toughness is represented by parameter called critical stress intensity factor K_{Ic} (D. Hayes, Fractography in Failure Analysis of Polymers, 2015). The stress intensity factor is a function of loading, crack size and structural geometry.

Mathematically stress intensity factor can be calculated as

$$k = \sigma \beta \sqrt{\pi a}$$

Where K is the stress intensity factor in MPa

σ is the applied stress

β dimensionless correction factor

a is the crack length

The fracture toughness affirmative real is defined as the critical stress intensity factor.

Fracture toughness is commonly tested by using specimen configuration that is single edge does not bend. In this test the thickness of the material is required to exceed some critical thickness as it is the

defining factor to perform fracture toughness (D.Hayes, Fractography as a Failure Analysis Tool, 2015).

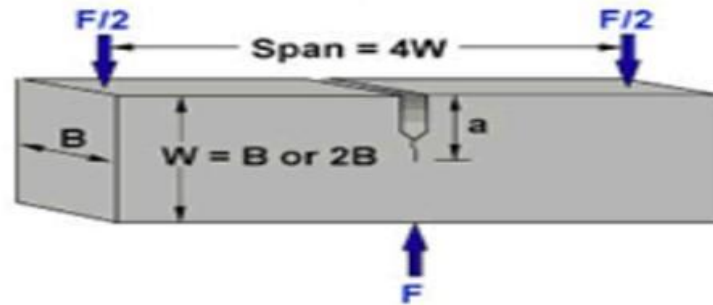


Fig.7 Flexural test schematics

1.5.3. Thermal Properties

Thermal property represents that how material reacts towards a change in temperature in its surrounding. Ceramic oxides do not conduct heat as well as most metals do. The thermal property of ceramics depends on the bond present i.e. covalent and ionic bonds, as there are not enough free electrons present. Ceramics depends on the following thermal properties that is heat capacity thermal expansion coefficient and thermal conductivity. That is why ceramics are used as insulating materials in a wide range of application.

The ability of the material to absorb heat from its surroundings is defined as heat capacity. During this process the atomic vibrations are affected by the vibrations of the adjacent atoms through bonding. These vibrations are transmitted across the material. The conduction of heat through a solid involves the vibration of atoms thus transferring energy (Faoite, 2012).

Thermal conductivity is the ability of a material to conduct heat. Thus, the amount of heat that passes through the solid material when there's a difference in temperature between one side of the material and the other while thermal insulation is the material's ability to reduce this heat transfer (Silvestre,

2015). Thermal conductivity depends on the defects present in the material. The transmission is interrupted by grain boundaries and pores thus making them a better insulating material (Bishui, 2014). Factors that affect the thermal properties of a ceramic are internal porosity, impurities, and grain boundaries.

$$\Delta Q / \Delta t = \lambda S \frac{\Delta T}{\Delta x}$$

where

ΔQ is the heat, Δt is the change in time, λ thermal conductivity, S is the surface area $\Delta T/\Delta x$ is the temperature gradient.

Thermal expansion is defined as the increase in volume and size of the material when heated.

$$a = \Delta L / L_0 \Delta T$$

Where a is the thermal coefficient, ΔL is change in length, L_0 is the initial length and ΔT is the temperature rise.

1.6.Motivation

Alumina being widely used due to its unbeatable combination of low cost with high mechanical properties. Instead of opting materials of high cost, this material can serve the purpose in various applications. Alumina is widely used in wear-resistant ceramics. It is three times cheaper than silicon carbide and four times cheaper than tungsten carbide. Thus, being cost effective, its usage in curved piping, in reducers, and nozzles etc. for commercial applications can be promising. The motivation of this thesis is to fabricate alumina at lower sintering temperatures than conventionally used. This is expected to reduce the manufacturing costs of alumina.

1.7.Objectives

The aim was to make a preliminary study of alumina for achieving its densification at a low temperature i.e., below 1600°C temperature through pressure-less sintering, and to achieve enhanced mechanical properties, making it cost effective for the commercial purposes. Thus, a route was selected which constitute the addition of sintering additives in small proportions in alumina matrix under the optimized conditions of temperature and compositions.

Chapter 2

Literature Review

2.1. Alumina

Alumina (Al_2O_3) an important raw material for traditional ceramics. It occurs naturally in its crystalline polymorphic phase as mineral corundum; these form the precious gemstones ruby and sapphire which are mixed in the earth's crust over billions of years by complex geological processes. Alumina has been attracting most of the attention as it is both an industrially important structural material and a model material for fundamental studies. (*T.Khalil, 2000)

Alumina comprises of non-equilibrium forms of partially hydroxylated aluminum oxide. Alumina is produced by bauxite Using Bayer process, Bauxite is treated with caustic aluminate solution containing soda, the dissolution reaction is carried out under pressure a temperature ranging from 140 Celsius to 280 °C. Impurities are removed thus leaving a clear solution, the hydroxy group precipitates, using an electric furnace. It has been one of the most widely used ceramics for industrial purposes owing to its exceptional properties such as high elastic modulus, corrosion resistance, high refractoriness, retention of strength, and thermal stability. Alumina used extensively in various filed, increases it's demand its melting point is as high as 2000 °C. Some specific applications where achieving high density is required, makes the use of alumina a bit difficult. (*T.Khalil, 2000) (CBE, 1999)

2.2. Structure of Alumina

Alumina possesses a strong alkalinity, broad range of surface area and notable iron exchange abilities. Alumina has the stable state known as alpha alumina, along with other forms of metastable alumina structures. Alumina crystal structure is called corundum structure, which consists of closely packed planes (A&B planes) of large oxygen ions stacked in a sequence.

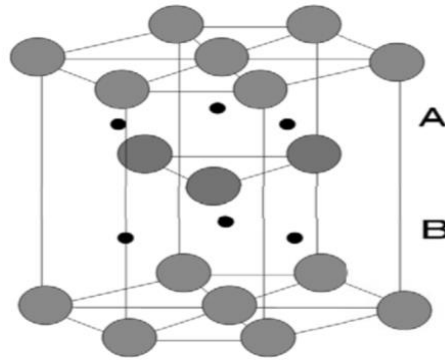


Fig.8 Structure of Alpha alumina, the grey spherical represents aluminium ion while black dots represents oxygen ions

There will be two Al^{3+} ions for every three O^{2-} ions. This helps in maintaining electrical neutrality of alumina.

2.3.α- Alumina

α- Alumina powder produced by Bayer method gives maximum purity up to 99.9%. high purity α- Alumina. The demand of high purity α- alumina is increasing because of its high stability and strength at high temperature. α-Alumina manufacturing is done by calcination by using aluminium hydroxide and alum, crystal transformation of α- phase occurs at high temperature exceeding 1200 °C joints are formed which are broken and to find particles through grinding. The grinding can take place via ball mill, vibration mill and jet mill in order to obtain monodispersed particles. Grinding has a great effect on the characteristic of the particle thus it affects the surface of high purity α- alumina powder. The unit cell is an acute rhombohedron of side length 5.2Å and plane angle ~55°.

2.4. Ceramography

It is the art and science of preparation, examination, and evaluation of ceramic microstructures. Ceramic powders obtained through various processes which involve methods such as synthesis of powder, mixing, grinding, shaping, sintering by diffusion or by formation of intergranular-liquid phase and cooling methods. The shaping of ceramics is a method through which the ceramic powder is compacted into desired shape by isostatic and axial dry pressing, extrusion, injection etc. which is known as green body having high porosity and poor mechanical properties.

To increase the mechanical properties, it is then subjected to sintering at various temperatures, which helps in the densification of the material as additive is either removed or diffused helps in shrinkage of the green body. The main objective is that this shrinkage should be as uniform as possible else contractions generates stresses that cause cracks in the material.

The control of particle size and impurities, refinements in processing methods, and blending with small amounts of other ceramic ingredients, can help in increasing the mechanical properties of the ceramic compared to its natural counterpart as these aids in achieving high particle packing and low porosity. The compaction of the green body after sintering at high temperature should be homogenous in order to avoid microstructural defects once it is sintered. Similarly, to increase the strength and toughness of alumina additives had been added. Alumina also has good hardness, low thermal conductivity, and good corrosion resistance.

The microstructure includes most grains, secondary phases, grain boundaries, pores, micro-cracks, structural defects, and hardness micro indentions. Most bulk mechanical, optical, thermal, electrical, and magnetic properties are significantly affected by the observed microstructure. The fabrication method and process conditions are generally indicated by the microstructure. The root cause of many ceramic failures is evident in the cleaved and polished microstructure. (Quesada, 2019)

2.5.Sintering

Sintering also known as frittage, it is a process in powder metallurgy in which the compacted material, in green, is subjected to a sufficiently high temperature and pressure thus forming a solid mass without

melting to the point of liquefaction. It is the bonding of particles at higher temperature. The mechanism of sintering is that the mass transport i.e., atoms diffuse across the boundaries or interstices between the particles, which occurs by the driving force i.e, reduction in surface energy. Small particles have high surface area than coarse particles (BARMORE, 1965). Once the process of sintering takes place, the compact thus obtained its densification changes. This occurs since during sintering the porous phase becomes discontinuous and is eliminated, at large but a few traces of occluded pores might be left behind. The initial density of the piece in green is usually 40–60% of the theoretical density, while the final density is 85–100%.

Sintering occurs either by surface transport or bulk transport. As sintering takes place a neck is formed between the two particles. At low temperature surface transportation dominates, shrinkage does not occur neither densification. Only mass production occurs which is eventually eliminated at surface. (Burke, 1976) While at higher temperature, bulk transportation, mass originates at the particle interior and deposits at the neck, thus causing densification and shrinkage. Sintering process is limited by low mass productivity thus making it non feasible.

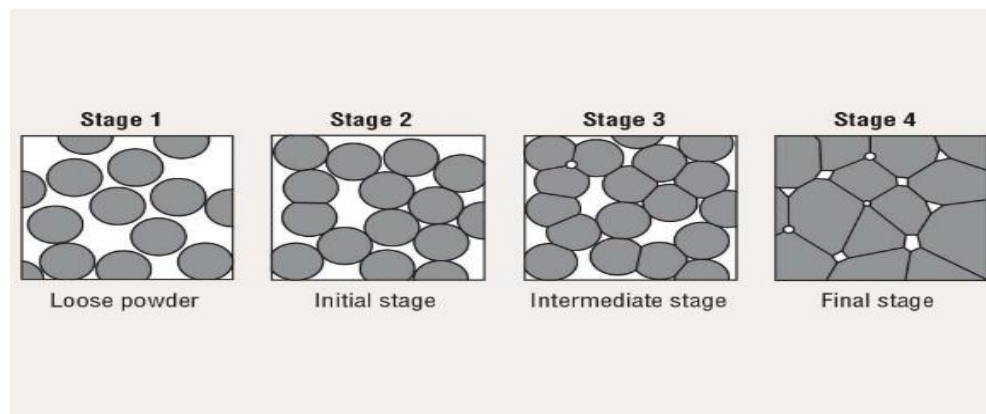


Fig 9 . Represents the sintering stages

Sintering can take place through three mechanisms:

2.5.1. Solid state sintering

It is a process of bond formation and densification of particles when heat applied is below the melting point of the material. no liquid is present rather joining of particles occurs by atomic diffusion thus reducing porosity. As the internal surface area occurs thus reducing surface free energy of a sintering compact, which is considered as a driving force. Sintering occurs at a reasonable rate as distance that matter has to be transported is small at higher temperature.

Initially as soon as some atomic mobility is achieved, sharply concave necks form between the individual particles. in intermediate stage the microstructure consists of interpenetrating network in three dimensions of solid particles. This leads to grain growth which is prominent in final stage. (GERMAN, 1996)

2.5.2. Liquid phase sintering

It is an important conventional sintering process at industrial scale when dealing with the fabrication of ceramics, especially those ceramics which poses a high degree of covalent bonding. This process in powder metallurgy entails the coexistence of solid and liquid phase, during which additive melts or reacts with small part of the major component to form eutectic, this allows the enhancement in densification, accelerated grain growth or producing grain boundary properties of the compact at lower temperatures. In case of applications where structural properties required liquid phase sintering is not much preferable. (GERMAN, 1996)

In liquid phase sintering an additive which is a small amount of liquid present in a very little volume percent of the original solid mixture, during sintering. The liquid can be formed either by the formation of low melting eutectic between the solid phase and liquid additive or through simply melting of additive. The liquid phase remains present during the whole process known as persistent liquid phase. It is necessary to have low solubility of liquid component in solid phase in persistent liquid phase, helps in attaining fully dense compact material (J.Svoboda, 1996). The liquid phase can be present for certain time during the sintering process known as transient liquid phase, this depends on the solubility ratios between solid and liquid phase and the temperature known as critical temperature that allows

liquid phase to exist at a specific time during sintering process. The sintering mechanism however is enhanced because the diffusion and mass transfer are fast than solid state sintering.

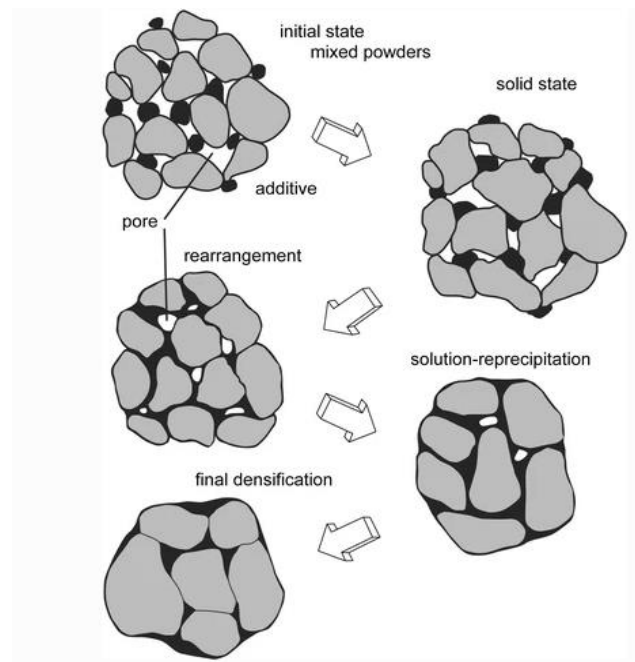


Fig.10 Different stages of liquid phase sintering

In liquid phase sintering, the dominant stages include

- a. Melting and redistribution of additive
- b. During capillary stress rearrangement of solid phase
- c. Shape accommodation of solid phase
- d. Densification driven by porosity.

There are three main characteristics controlling the liquid phase sintering.

2.5.2.1. Wetting

The surface tension is the property of liquid surfaces, exists when two surfaces are present. It is a contractive tendency of the surface of the liquid in contact with the other surface at the boundary between the two, which measures the surface free energy of liquids. The surface tension between solid and liquids cause to generate capillary forces. Due to which strong attractive forces rises between the neighboring grains. Those liquids which have low surface tension give rise to small contact angles thus the phenomenon of wetting takes place at the boundary of the two phases. The liquid surface phase the tendency to wet the solid if the cohesion between liquid molecules is smaller than the adhesion between the liquid and solid at the boundary, thus it can be said that liquid has the tendency to wet the solid. (Huhtamäki, 2018)

Mathematically

$$\Gamma_{sv} = \gamma_{sl} + \gamma_{lv} \cdot \cos\theta$$

Wetting is promoted if Γ_{sv} i.e. solid/vapor value is high and γ_{sl} i.e. solid/liquid and γ_{lv} i.e. liquid/vapor values are low. The contact angle ' θ ' plays an important role in wetting of the solid. If the contact angle is less than 90° or 0° wetting value is high, if the angle is greater than 90° than wetting will be minimum, in this case the sintering will occur by solid phase mechanism. (Huhtamäki, 2018)

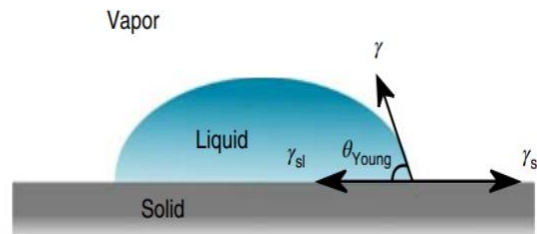


Fig.11 Wetting on the solid surface

2.5.2.2. Dihedral angle

Another condition that effects the liquid phase sintering is the distribution of liquid over a solid particulate to cover the surface to its maximum capacity. This can be observed by calculating dihedral angle, it is the angel between solid liquid interfaces. This represents the penetration and separation of the grain boundary by the liquid.

Mathematically

$$\Gamma_{gb} = 2\Gamma_{sl} \cos(\psi/2)$$

Where Γ_{gb} is a grain boundary energy, Γ_{sl} represents energy at the solid/liquid interface and ψ is a dihedral angel. The dihedral angle is independent of the pressures in the phase. If the dihedral angel is 0° than the liquid will penetrate completely, but as the dihedral angle increases, the liquid phase penetration decreases. It is important to note that the grain boundary energy must be less than solid/liquid interface surface energy. (Huhtamäki, 2018) (Randall M. German, 2009)

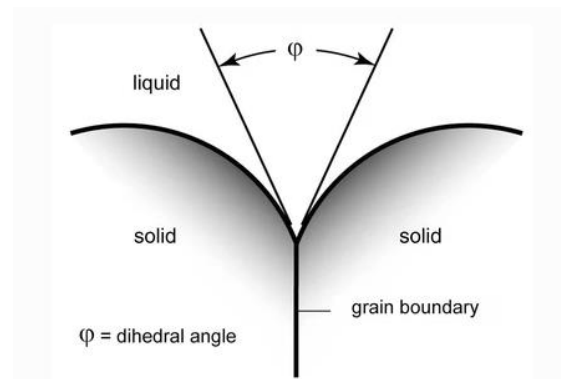


Fig.12 Complete penetration of liquid when dihedral angel is 0°

2.5.2.3. Solid solubility in liquid

The solubility affects all stages of liquid phase sintering. The higher solubility of the components present in the solid phase and liquid phase determines the liquid phase as persistent or transient. This is defined by solubility ratio, as it not only defines the persistent or transient nature but also affects the factors such as rearrangement of solid particles, densification, and solution precipitation. The

solubility effects the initial shrinkage and swelling prior to rearrangement, as mass transfer occurs accompanied by dimensional changes.

The most beneficial state of solubility is unipolar solubility in order to achieve high densification in persistent liquid phase. In this system the solubility of the liquid forming component in solid is low while solubility of solid forming component in liquid is high. (Randall M. German, 2009)

For transient liquid phase the condition is reversed i.e., the liquid forming component in solid is high while the solid forming component in liquid is low. This helps in densification of the compact. (Huhtamäki, 2018)

An unbalanced diffusivity between the additives and the green compact effects the microstructure of the sintered body. The relation of additive and the base can be given as diffusivity ratio

$$D_R = \frac{D_B}{D_A}$$

Where D_R is diffusivity ratio, D_B is diffusivity of base and D_A is diffusivity of additive.

The solubility of the liquid defines the densification of the compact. limited densification means the system is insoluble.

Solubility ratio is given by

$$S_R = \frac{S_B}{S_A}$$

Where S_R is solubility ratio, S_B is solubility of base and S_A is solubility of additive. It should be noted that higher the solubility ratio has effect on porosity and volumetric solubility.

2.6. Stages of liquid phase sintering

The liquid phase sintering occurs in three stages, as study shows. Classically, the stages of liquid phase sintering is as follows

- Particle rearrangement
- Solution-reprecipitation
- Solid-state sintering

2.6.1. Particle rearrangement

When compact is subjected to heating, rearrangement of particles takes place in the first stage. The liquid is formed, densify

Swelling is apparent and occurs rapidly, particles due to capillary forces in liquid phase sintering, the solid particles movement occurs from their initial position towards the arrangement of dense packing randomly, which helps in filling the spaces thus eliminating pores. This helps in achieving densification during the shrinkage period (Kingery W. D., 1959) . The process is rapid, and it can be observed by Kingery's model i.e.

$$\Delta L/L_0 \approx 1/3 \Delta v/v_0 \approx t^{1+y}$$

or can be observed by analyzing capillary forces between the particles separated by liquid layer.

2.6.2. Solution-reprecipitation

This is the second stage in which solution precipitates while rearrangement of particles decreases significantly. Chemical potential generated by capillary forces at point of contact is responsible for the dissolution of atoms at point of contact, which are reprecipitated at areas far from point of contacts

thus causing shrinkage and densification. the most essential condition for this process to occur would be good wetting of the solid and finite solubility of solid in the liquid. Along with densification, coarsening can also occur during dissolution and reprecipitation. This whole phenomenon contributes in particle arrangement, grain growth and shape accommodation.

Contact flattening theory and pore filling theory well explains the densification process during the liquid phase sintering. Kingery proposed contact filling theory which states that shrinkage occurs, mass transport from contact area between grains to the non-contact area i.e., neck region occurs thus forming contact region between the particles flat. This process induces continuous grain shape change till the point of complete elimination of pores. (Kingery W. D., 1959)

The other mechanism i.e., pore filling theory was proposed which states that pores are eliminated through filling by the liquid. In this case microstructural homogenization occurs when prolonged sintering takes place as material deposition occurs at the liquid pocket, which begins at the surface towards the liquid pocket center. This process is known as Ostwald ripening process. This gives homogenized surface. (Kingery W. D., 1959) (Petzow, 1984)

2.6.3. Solid-state controlled sintering

The final stage of the process in which overall shrinkage occurs and densification of the compact is reduced due to the formation of the structure which inhibits further rearrangements. Coarsening i.e. precipitation of particles embedded in a system dominates in this step. The rate of this depends on the diffusion through liquid and solid.

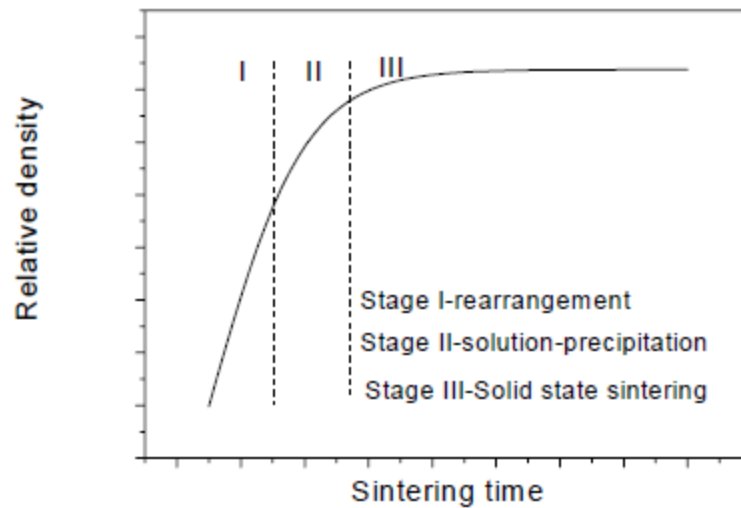


Fig.13 Schematics of change in densification wrt. sintering time

2.7.Sintering Additives

Historically, alumina was being sintered through means like high pressure and pressure less sintering. However, a new approach was envisaged in 1900's whereby different additives, including either metal or non-metal-based oxides or glassy oxides, were considered for sintering of alumina which resulted in cost effective and economical sintering process. The amalgamation of these additives with alumina enabled the scientific community to attain densification of alumina at low temperatures. This makes it safe to assume that additives are the prerequisite for densification. The quantity and type of the sintering additive being added to the alumina are the baseline to determine the liquid forming temperature, the commencement of densification and its rate during sintering. The determination of characteristics like grain-morphology or grain boundary phase are also defined by them, which in turn play vital role in maintaining the high-temperature properties. In order to achieve densification of alumina, the prioritized additives are metal oxides which deter the formation of solid solutions in specific composition i.e. the binary metal oxides or ternary metal oxides like CuO, TiO₂, B₂O₃, MgO

Extensive work is being performed for pressure-less sintering of alumina as additives are added thus resulting of densification at low temperatures.

- a. The effects caused by variety of sintering additives encompassing MnO_2 , SiO_2 , TiO_2 and MgO , on the densification as well as micro-structural evolution /development of alumina powders, obtained as residue during the Bayer process, were studied by H. **Erkalfa et al** (Erkalfa, 1996). The colloidal technique was implemented to ascertain the homogeneous integration of alumina powders and additives. Furthermore, the quality of the powders was improved through the process of calcinations, hot washing, and re-calcinations. The process entailed achievement of microstructures with densities ranging between 90-96.7% of the theoretical density. It was inferred that strength values as high as 180- 380 MPa, along with a homogeneously distributed finer grain size was obtained through the addition of 1.5% MnO_2 - 0.1% TiO_2 - 0.5% MgO - 2% SiO_2 . It was further concluded that where B_2O_3 played vital role in enhancement of the sintering process, the MgO along with improving the microstructure uniformity, also suppressed the discontinuous growth of grain. These additives played part in enhancement of the mechanical properties along with lowering the temperature requisite for sintering.
- b. A maximum of 95 percent theoretical density at firing temperature of 1400 °C/ 4 hours was observed by **A Bettinelli et al** (Botinelli, 1988) during investigations conducted for determining the effect of adding optimum amount of 2.25 wt% of CaSiO_3 on the densification of undoped α alumina. it was also inferred whilst investigation of the densification kinetics that density of samples remained un-affected upon addition of transitional metal oxides containing a low melting flux (i.e. TiO_2 , Nb_2O_5 , MoO_3) to alumina.
- c. A reduction of the residual glassy phase can improve the mechanical behavior of alumina obtained by (liquid phase sintering) LPS. Thus, the use of a glass-such as a glass-ceramic-that encourages sintering during heating and crystallizes in stable phases during the cooling cycle may be an alternative way to obtain high density alumina by LPS, while simultaneously producing a large amount of crystalline phase in the grain boundaries¹⁹. In addition, less grain growth and less residual glassy phase could be obtained. The influence of a Li_2O - ZrO_2 - SiO_2 - Al_2O_3 (LZSA) glass-ceramic on the mechanical behavior of alumina was observed. An

increase of 37-177% in the fracture energy due LZSA addition in the alumina was achieved for the range of grain size (Montedoa, 2018).

- d. **Coble** (Coble, 1997), inferred that near theoretical density of alumina can be achieved through addition of magnesia (0.25 wt%). Myriads of mechanism have been suggested in a range of literatures that grain growth can be inhibited and densification can be enhanced by using MgO . it has also been observed in literature that by increasing the value of grain boundary diffusion coefficient, MgO increases the rate of densification. Additionally, it has also been reported that enhanced densification through the use of MgO is achieved due to lowering of the surface diffusion. There is enough evidence in several studies to accept that suggest MgO deters pore boundary separation by lowering the grain boundary mobility, thereby entailing a decrease in grain growth rate. However, the exact mechanisms to how magnesia addition enhances densification still remain controversial.
- e. **Radonjić et al** (Radonjić, 1997), whilst studying the effect of MgO doping on the densification, as well as on the grain growth of alumina observed an increase in the densification kinetics but decrease in the grain growth rate of alumina. It was observed that whence magnesia addition could decrease the particle size during phase transformation, it could decrease grain growth during sintering.
- f. **Atsushi Odaka et al** (Odaka, 2008), demonstrated that Ca doped alumina nano-powders were able to produce fine-grained ceramics. The nano-powders were obtained using CaCl₂ and polyhydroxoaluminum (PHA) solutions through a sol–gel route under α -alumina seeding. Appropriate composition for producing the above for low-temperature finer grained densification were 0.10 mol% Ca-doping, 5 mass% α -alumina seeding. This was followed by calcinations carried out at a temperature of 900 °C. this resulted in the formation of new nano-sized alumina powders, consisting of α -alumina particles and nano-particles with 80 nm as an average grain size. These Ca-doped nano-powders were used to produce uniformly micro-structured and fully densified alumina ceramics with an average grain size of 0.66 μ m temperature as low as 1375 °C. this emphasized the suitability of the proposed sol- gel route for preparing Ca-doped nano-powders for fabrication of dense and fine-grained alumina

ceramics. Undoped samples with 5 mass% seeds had a microstructure with an average grain size of 1.39 μm at 1375 $^{\circ}\text{C}$.

- g. **R. Voytovych et al** (Voytovych, 2002), studied the impacts on grain growth and densification of very high-purity α -alumina by doping it with varying amounts of yttrium spanning between 0 to 3000 wt% ppm of yttria and subsequently sintering the sample at 1450, 1550 and 1650 $^{\circ}\text{C}$. It was observed that effect of yttrium doping showed inverse relation with temperature increase, as sample exhibited densification and coarsening at 1450 $^{\circ}\text{C}$, but had very little effect at 1550 $^{\circ}\text{C}$ and no effect at 1650 $^{\circ}\text{C}$. This variation in densification behavior is inferred to be caused due to the transition of densification control source from grain boundary diffusion to lattice diffusion with increasing temperature. It was also observed that the coarsening rate increases more expeditiously with temperature as compared to the densification rate. This was said to be correlated with the higher measured activation energy for grain growth than for the diffusion processes, which control the densification.
- h. **C. Ivan B. Cutler et al** (Cutler, 1957), inferred that sintering of alumina can be enhanced at temperatures below 1700 $^{\circ}\text{C}$ by using both small particles and the addition of certain oxides. The sintering temperature for under consideration 96 % dense alumina bodies was curtailed up to 1300 $^{\circ}$ to 1400 $^{\circ}\text{C}$ range by varying combinations of small particle size and oxides. The cause for reduction in sintering temperature was deduced to be the formation of a liquid phase. Thin sections of the alumina sintered at low temperatures when observed revealed bodies with small grain size with bulk densities above 3.80 g/cc.

2.7.1 Material choice as sintering additives

2.7.1.1 Copper oxide (CuO)

Copper oxide exists in two forms i.e. cupric oxide (CuO) and cuprous oxide (Cu₂O). CuO however is considered as a sintering additive that gives liquid phase when added in a system. Thus it causes liquid phase sintering, it mainly plays fluxing action, make atom easily move to membranes on alumina particles surface, and react with aluminum oxide.

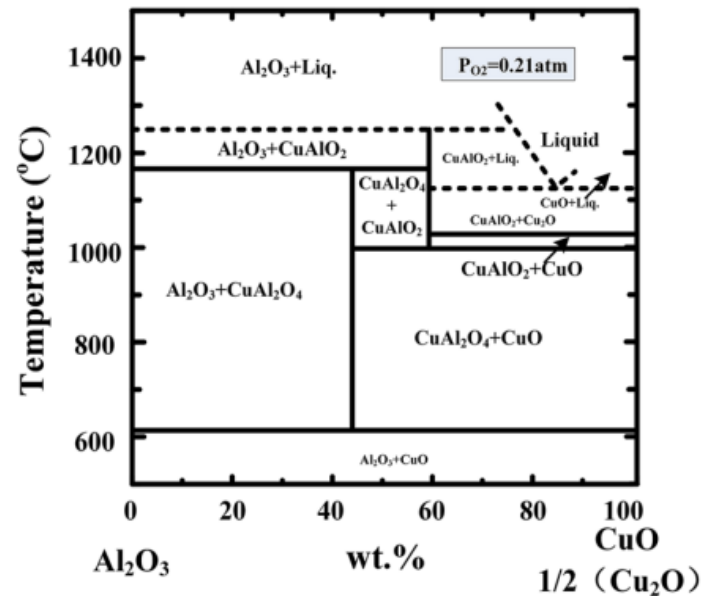


Fig.14 Phase diagram of alumina and copper oxide

Copper oxide and titania have been utilized in isolation as well as in combination with various oxides to maximize mechanical and structural properties of alumina.

S.Ramesh et.al (Sing, 2008) studied the effects caused by addition of CuO in Al₂O₃. It has been observed that the addition of CuO aids in the formation of liquid phase at the grain boundaries of alumina, resulting in decreased sintering temperature, and enhanced densification. Modification in morphology of the grain size and improvement in mechanical properties was achieved due to formation of CuAl₂O₄ liquid at grain boundaries which modifies the morphology of the grain and improves mechanical properties (Haldar, Effect of nano CuO addition on the tribo-mechanical behavior of alumina ceramics in non-conformal contact, 2020). The significance and effectiveness of CuO addition to alumina can be envisaged through the apparent decrease in porosity due to inter-diffusion of most grains, resulting in shrinkage and large size grains. It also improves fracture toughness and hardness by preventing grain growth. The phase transformation causes volume expansion around the crack tip. As a result, the neighboring grains experience compression and inhibit the crack movement. The toughening of the alumina matrix is a result of grain refinement and phase transformation.

Partha Halder et.al (Haldar, Effect of Nano CuO Addition on the Tribo-Mechanical Behavior of Alumina Ceramics in, 2020) studied the addition of copper oxide at nanoscale in alumina at low temperature. The effect of density was studied as sintering temperature was increased. the addition of copper oxide formed a liquid phase CuAl_2O_4 thus modifying the morphology of the grain, this in turns imparts effect on mechanical properties to be enhanced. The optimization of copper oxide was achieved to be 2wt% increasing the hardness and fracture toughness of the system.

2.7.1.2 Titania (TiO_2)

Titania occurs in three i.e. Brookite, Rutile, Anatase. The former is orthorhombic while the lateral two are tetragonal. Rutile however is the most stable one thermodynamically. Thus, rutile plays a significant role in industries. Titania when heat treated its forms changes from anatase to rutile, where anatase is a metastable state.

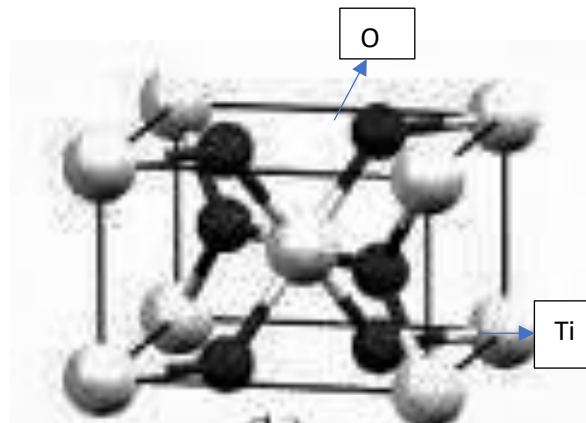


Fig.15 Titania (Rutile) unit cell, where black dot represents Oxygen and Ti is represented by white dots

When titania added in a system the mechanical properties changes by the composition and microstructure. Thus, due to various applications these properties of titania can be tailored, thereby entailing advantageous applications.

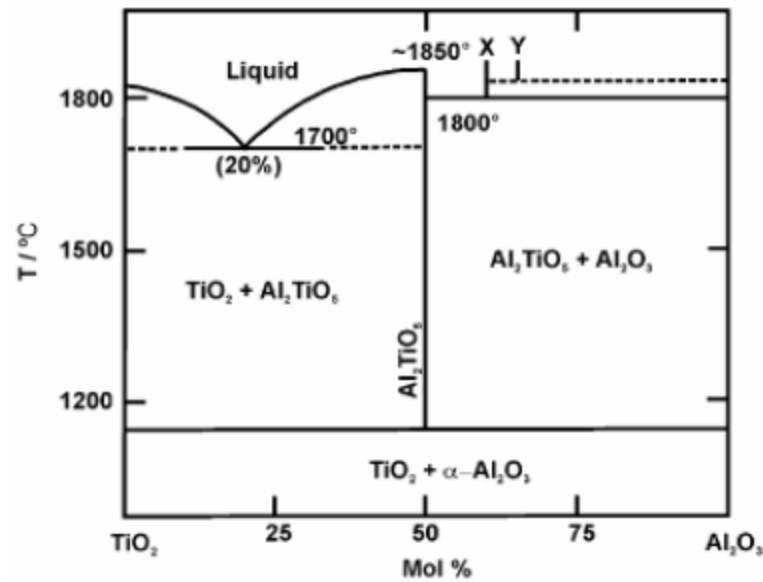


Fig.16 Phase diagram of Alumina- Titania system

Titanium dioxide can with aluminum oxide generation solid state reaction, make aluminum oxide realize sintering. Thus, when it is inferred that solubility of titania in alumina, determined by the lattice parameter shift of alumina, is quite low. Whilst analyzing the effects of temperature on solubility of titania in α -alumina, it was observed that it existed in solid form at 1150°C, and the solubility was 0.27% at 1300-1700°C. Surpassing solubility limit, excess titania coexisted with α - alumina as rutile below 1350°C and above 1450°C it co-existed as Al₂TiO₅. The addition of titania also promoted the grain growth of Al₂O₃. An inverse relation between grain size and increasing Al₂TiO₅ concentration was observed beyond the solubility limit. Al₂TiO₅ existing as a second phase deter the grain growth of alumina. (KUMARI, 2013)

Hori et al. (Us Patent No. 4,892,850, 1990) reported tough alumina-titania composite sintered body. The vapor-phase reaction of AlCl₃ and TiCl₄ by vapor phase reaction an alumina-titania composite powder was prepared. It was stated that composite body can be sintered at or under 1280°C and can achieve high density. The geometrically anisotropic particles imported crack deflection, thus deteriorated toughening mechanism of the sintered body.

Serkan A ball (SerkanAball, 2011) reported mechanical property of higher amount of titania in alumina (40 and 48 % TiO₂). The addition of titania causes variation in microstructure such as phase distribution, porosity, and hardness etc. According to this the micro hardness values of the alumina - 40 wt% titania are slightly higher than that of the alumina-48wt.% titania. It is shown that the micro hardness values are depends on the amount of titania.

2.7.1.3 Zirconia (ZrO₂)

SL. Xu & M.Chen et al. (Xu, 2015) has studied the performance and sintering behavior of high alumina refractory, based on the ternary subsystem. MgAl₂O₄-CaAl₄O₇-CaQl₁₂O₁₉ were investigated using to 8 wt.% of ZrO₂ as an additive by conducting solid state reaction sintering. it was observed that added ZrO₂ forms solid solution after dissolving in the ca6 grains in, resultantly causing enhanced isotropic growth of ca6 grains and consequently improved the sintering. result was improved densification process and more compact structure was observed in areas with enrichment of ZrO₂. upon further ZrO₂ addition, tetragonal ZrO₂ crystals were formed in the grain boundaries, which enhanced the thermal shock resistance by increasing the solid solubility limit, inferring that ZrO₂ addition exhibited a positive effect on sintering behavior and of this refractory. in addition, it is considered that the optimal amount of ZrO₂ addition was about 4% considering the performance together with the cost.

It has been seen that adding ZrO₂ promotes composites with higher densities. The density has been inferred to possess direct relation with increasing zirconia content and sintering temperature, while porosity possess inverse relation with the same variations of zirconia content and sintering temperature. SEM images visualize the microstructures of ZTA showing that the grains remain homogeneous and finer at 1550°C. It can also be observed that the grain size of ZrO₂ possesses inverse relationship with the increase of ZrO₂ content, whereas it increases with the increase of sintering temperature and hinders the grain growth of Al₂O₃ which contributes to the variation of porosity. Hardness and elastic modulus have been found to be increased with sintering temperature, while the addition of ZrO₂ decreases the hardness and elastic modulus of the composite. The flexural strength increases with increasing zirconia content as well as sintering temperature. The martensitic

transformation and frontal process zone are predominant mechanisms to increase the flexural strength of Al₂O₃- ZrO₂ composite. The zirconia substitution in pure Al₂O₃ and the change of sintering temperature was found to have a significant effect on structural and mechanical properties (Hossen M. , 2014).

Chapter 3

Experiment and Characterization

3.1 Experimental route

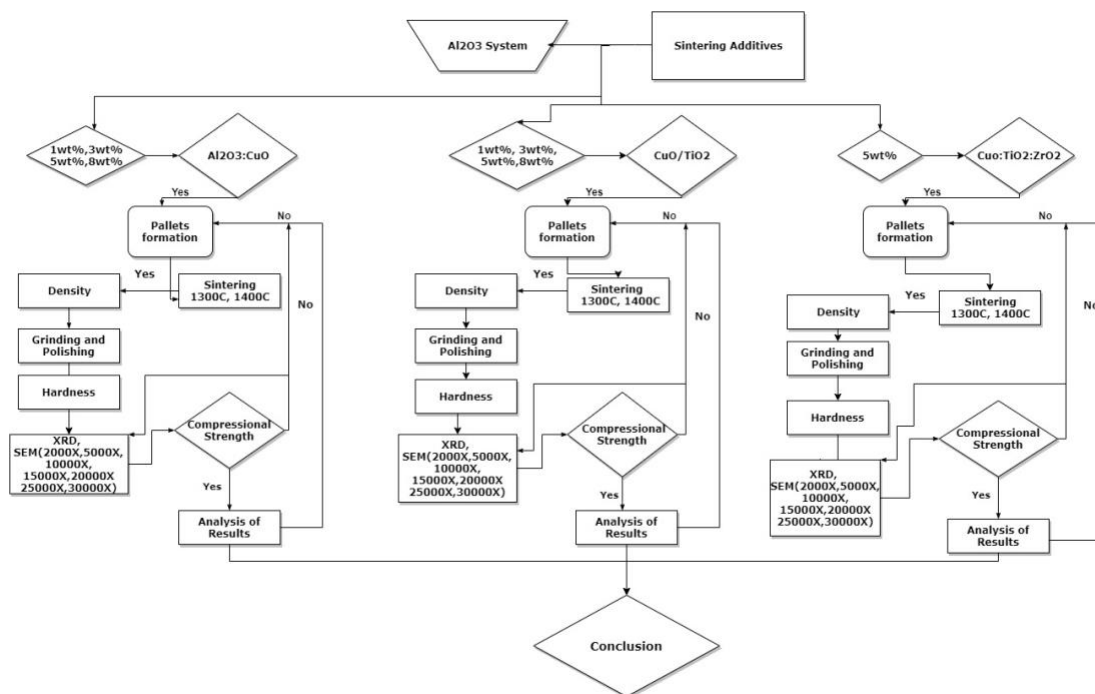


Fig.17 Diagram presenting layout of experimental work

3.2 Sample Preparation:

3.2.1 Synthesis of Copper oxide

The metal powder of copper, rusty orange in color was directly obtained. It was then subjected to heating in the muffle furnace for 2hr at 300°C for auto combustion of powder to get a black powdery mass. The burnt powder was then agate, ultimately to get copper oxide powder.

3.2.2 Material preparation and sintering

α - alumina in its high purity (99% pure) used as a base for composing the specimen. Its densification and mechanical properties are needed to be enhanced. The α - alumina was spherical in shape and had a size of 4 μ m -6 μ m.



Fig.18 Powder form α - Al_2O_3

3.2.2.1 Alumina: Copper oxide

The batches were prepared, initially, mixing of CuO in α - Al_2O_3 in various compositions were made i.e. 1wt%, 3wt%, 5wt% and 8wt%. Samples were marked as C1, C3, C5, C8 respectively. The wet mixing was carried out in ethanol and was subjected to the low energy ball milling for 12 hours. The powder to ball ratio was taken to be 1:10 for this purpose. The slurry obtained was dried at 100 °C for 2hrs. The powder was then crushed in pastel and mortar to get homogenous powder.

Table1. Represents condition for homogenous mixing of powdered samples

Sr. No	Ball ratio	Medium	Milling time	Drying time
1	1:10	Ethanol	12hr	1 hr

Pellets of the sample powders were prepared by using die of 12mm in diameter. The sample powders were then pressed isostatically using hydraulic press under a uniaxial load of 200MPa. The green body

was than sintered under ambient conditions with heating rate of 10°C/min at different temperatures i.e. 1300 °C and 1400 °C for 4 hours in a Naberthem Muffle box furnace.

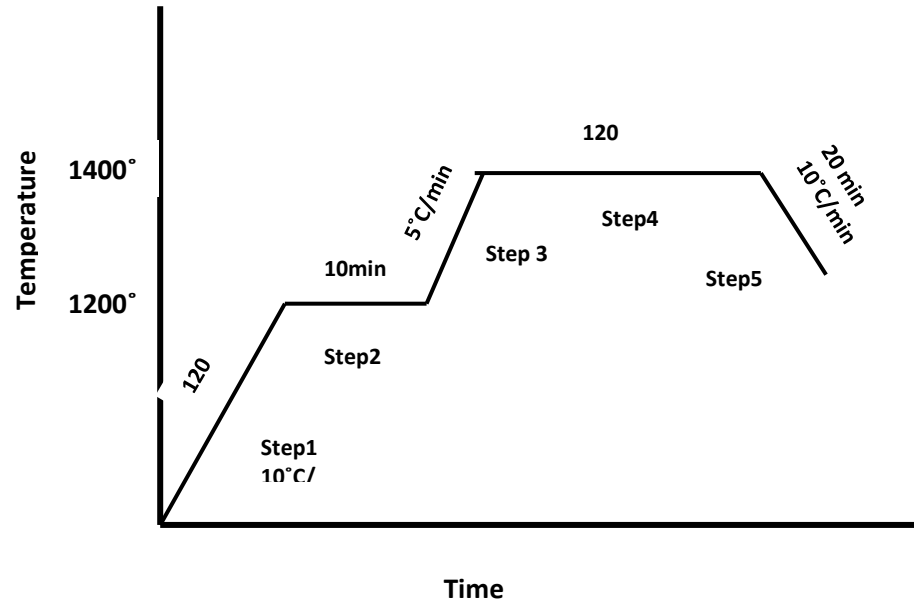


Fig 19. Temperature vs time graph of sintering

Further its characterizations were done. The temperature range was defined in this step to carry out further experiments

Table 2. Composition of Alumina system with addition of Copper oxide

Sr. no.	Al ₂ O ₃ Mass(g)	CuO	
		Wt%	Mass (g)
1	1.98	1	0.02
2	1.94	3	0.06
3	1.9	5	0.1
4	1.84	8	0.16

3.2.2.2 Alumina: Copper oxide: Titania

A new batch was prepared in which the composition of Cu was same as mentioned above but with it TiO_2 in powder form, was added as a sintering additive in Al_2O_3 . The concentration of TiO_2 was taken to be 2wt%. The powder was passed through the same process as forementioned. Prepared pellets were subjected to the sintering process and the temperature considered were $1300\text{ }^\circ\text{C}$ and $1400\text{ }^\circ\text{C}$. The characterizations were carried out. This was the step which helped in determining the composition of CuO to be considered in the further series of the experiment to be performed.

Table 3. Composition of Alumina system with Copper oxide-Titania

Sr. no.	Al_2O_3 Mass(g)	CuO		TiO_2
		Wt%	Mass (g)	Mass (g)
1	1.9	1	0.02	0.04
2	1.7	3	0.06	0.04
3	1.5	5	0.1	0.04
4	1.2	8	0.16	0.04

3.2.2.3 Alumina: Copper oxide: Titania: Zirconia

The previous step was determining step of the composition of CuO which turned out to be 5wt%, thus TiO_2 along with ZrO_2 , both in powdered forms, added in alumina was carried out. Where composition of ZrO_2 was 1wt% and 5wt%. This was determined by the help of literature review and series of experiments performed for its confirmation.

In the same previously mentioned manner, the powders were mixed in alumina, pallets were formed and sintered at $1300\text{ }^\circ\text{C}$ and $1400\text{ }^\circ\text{C}$ for 4 hours in muffle furnace. Sintered pallets were subjected to various characterizations to determine the change in mechanical properties of the prepared samples and its effect on the densification of alumina.

Table 4. Composition of Alumina system with addition of Copper oxide-Titania- Zirconia

Sr. no.	Al ₂ O ₃ Mass(g)	CuO Wt%	TiO ₂ Wt%	ZrO Wt%	
1	1.2	5	2	1	5

3.2.3 Mounting

For holding sample bakelite powder was used. A pressure of 280 bars was applied and the curing time was set at 180 °C.

3.2.4 Grinding

The sintered pallets prepared in all above mentioned scheme, when once mounted, were subjected to grinding. The sand paper with grit size of 600, 800,1000,1200 and 1800 respectively. The sample orientation was rotated to 90 °C to ensure proper orientation of scratches.

3.2.5 Polishing

Alumina powder of 0.5 size and diamond paste of 1 micron size were used in the form of slurry, separately to gain better results. The samples were subjected to polishing for obtaining smooth surface.

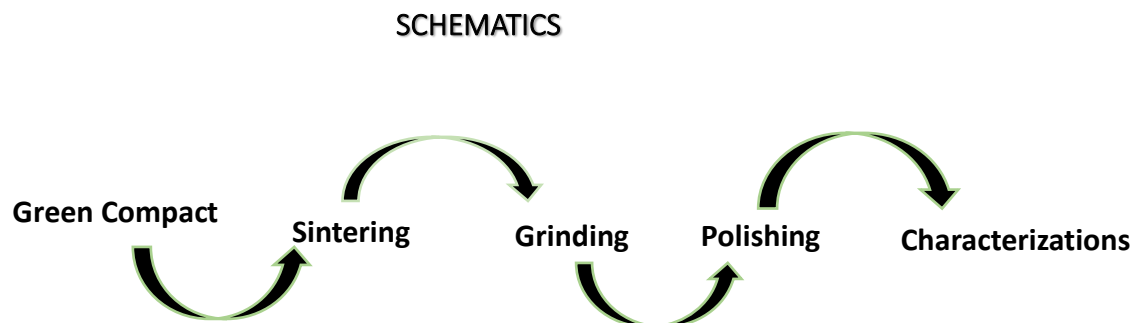


Fig20. Represents the general schematics of the experimental works

3.3 Characterization techniques

The techniques used for the characterization of prepared specimen are

- X-ray Diffraction (XRD)
- Scanning Electron Microscopy (SEM)
- Density measurement
- Vickers hardness
- Universal Testing Machine (Shamizdu AG-X plus) (UTS)

3.3.1 X-ray diffraction (XRD)

X-ray diffraction is an analytical technique primarily used in material science to determine the information on unit cell dimensions, phase identification and crystallographic structure and physical properties of a material (Bunaciu, 2015). Max von Laue noble prize winner on his work on X-rays diffracted by the solid crystal system.

The seven crystal systems are

- Cubic (isomeric)
- Tetragonal
- Triclinic
- Orthorhombic
- Hexagonal
- Monoclinic
- Trigonal

This technique is based on the determination of angles from constructive interference and destructive interference of monochromatic x-ray (Bunaciu, 2015). The principal is used is known as Bragg's law in which crystal atoms scatter incident X-rays through interaction with electrons of the atoms. Bragg's law is given as

$$2d\sin\theta=n\lambda$$

Where d is the spacing between diffracting planes, θ is the incident angle, n is the integer and λ is the wavelength

The range for the wavelength of X-rays applied for analysis is from 10Å to 2.5 nm. It consists of five main components,

- Radiation source
- Sample holder
- Component to limit wavelength range of received radiations
- Radiation transducer
- Signal processing and read out component

In most of the diffractometers, the assembly of the X-ray source is in such a way that it is placed along with the detectors at the same side of the sample. During the process the incident rays strike at some angle which are then reflected and are passed onto the detector. Electrons are generated in cathode ray tube by the filament which is heated. Electrons are then accelerated along with the direction of target towards target when electric field is applied (CivanPhD, 2016). Characteristic X-rays are produced when these electrons strike the inner shells of the target material. Then this monochromatic X-ray beam is directed to fall on the sample. The angle is maintained by the unit called goniometer. Scintillation counter is the most commonly used detector which records the intensity of reflected X-rays obtained by constructive interference. The complete scan range of powder x-ray diffraction ranges from 5° to 150° .

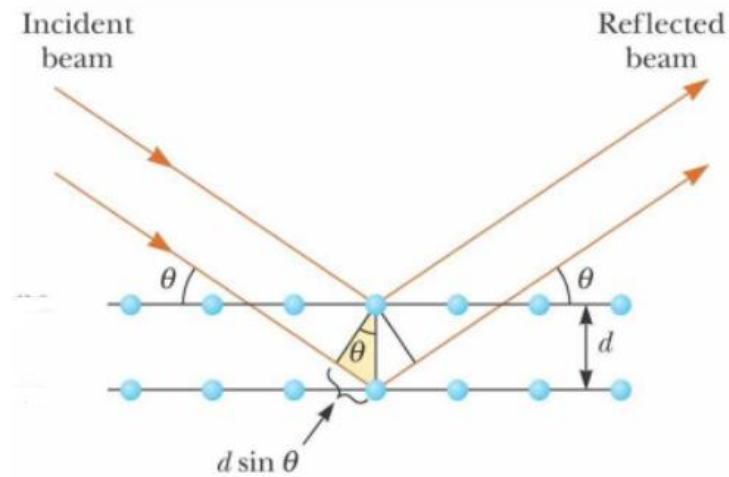


Fig.21 Diffraction of light beam demonstration

3.3.2 Scanning Electron Microscope (SEM):

Scanning electron microscopy is a technique used for the investigation of morphology of materials, crystallography, and orientation of planes. Manfred Von Ardenne designed SEM for the first time in 1938. Metals, nonmetals, ceramics materials etc. can be analyzed though the sample to be analyzed by SEM should be conducting, but if not a thin layered coating of gold or graphite is done to make non-conducting samples conductive in order analyze it (Seiler, 1983). A high energy electron beam is bombarded on the material under analysis to produce 3D image with a resolution up to 1nm. Degree of magnification is controlled by electromagnets. Surface of the material is focused by a fine beam of electrons. As a result, electrons or photons are knocked out of the surface and directed towards detector. The output from the detector modulates the brightness of the cathode ray tube. For every point where electron beams are focused and interact, it is plotted on consequent points on cathode ray tube. As a result, 3D image of the material is produced.

The electron interacts with the specimen in following ways

- a. Back Scattered Electrons
- b. Secondary Electrons

- c. Augers Electrons
- d. Characteristic X-ray

These interactions mainly depends on the penetration of the beam through the surface of the specimen. Secondary electrons is commonly used in SEM mode. These electrons are emitted near sample surface which results into formation of image.

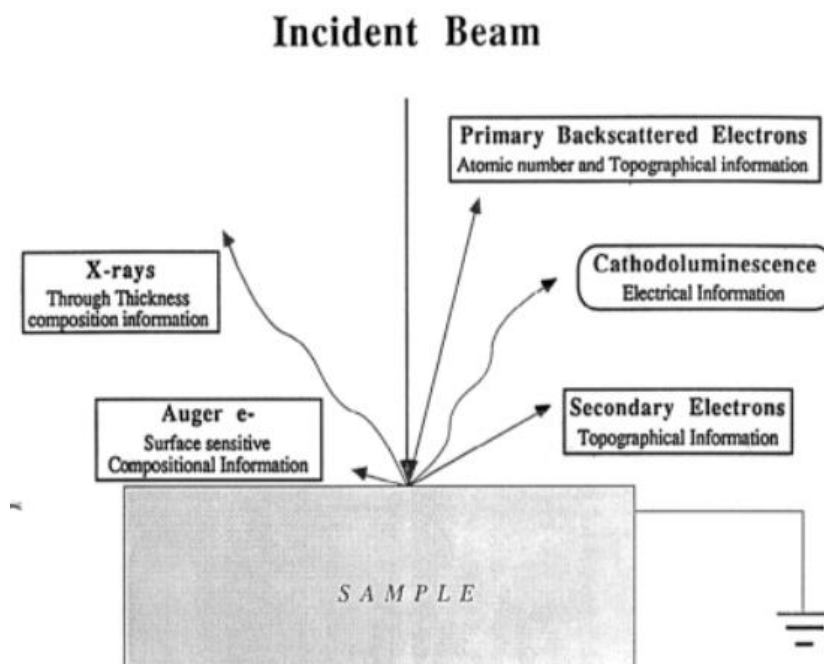


Fig.22 Schematics of sample interaction during SEM

3.3.3 Density measurement

Density is the measure of the compactness of a specimen. Density of the material can be determined by Archimedes principle. This states that when a specimen is immersed in a liquid an upward force acts upon it known as buoyant force, due to the pressure built at the downward side is equal to the weight of the fluid that was displaced by the immersed specimen (Lowell, 2004). The bulk density was calculated by the following formula

$$\text{Bulk Density} = \frac{\text{Dry weight}}{\text{soaked weight} - \text{suspended weight}}$$

The apparatus used for measure weight is shown below in Figure



Fig.23 Densification measurement apparatus

3.3.4 Micro- Vickers Hardness

Hardness, applied to most materials, is a commonly employed mechanical test. The information obtained can complement or used in conjunction with other materials verification techniques. In 1921, vicker hardness test was developed by Robert L. Smith and George E. Sandland. The prupose was to overcome the drawbacks in the refinement of test results, when performed by the Brinell hardness testing. This is used for all the metals present in the universe. In this method the indenters play an important role. The indentation is made on the test material with the help of a diamond indenter. It has the shape of a pyramid with square base and angle of 136° between opposite faces. The angle is 22° between the flat surface and the inclined outward face of the diamond (Ullner, 2001) . The force

subjected on to the aerial is between 1gf and 100kgf. The load applied on the material is between 10 to 15 seconds. As the load is removed the mark i.e. the two diagonals of the indentation left in the surface of the material (Ghorbal, 2017) . The area of the sloping surfaces is calculated using microscope.

The procedure for calculating the hardness of the material was

- a. Sample was placed on the stage of Vickers hardness tester
- b. The settings were adjusted to zero and observed through microscope
- c. Indent in-placement and load applied
- d. Removal of load
- e. Measurement of the dimensions of the indent formed through optical microscope
- f. Calculation of Vicker hardness number

Vicker hardness mathematically calculated as

$$HV = \frac{2F \sin \frac{136}{2}}{d^2} \quad HV = 1.854 \frac{F}{d^2} [kgf/mm^2]$$

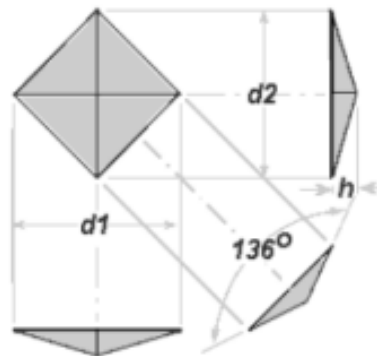


Fig.24 Schematics of indent in Vickers hardness apparatus

3.3.5 Universal Testing Machine (Shamizdu AG-X plus) (UTS)

In 1880, the first UTS machine was developed in order to perform the tensile and compression testing for the material. This gives an intensive study about the physical and mechanical properties of the specimen by measuring and analyzing the performance of the material under the applied force.

The compression testing of the materials helps to determine the materials behavior when it is subjected under the applied crushing load. The relationship between the stress and strain graph is the same as for the tensile loading. Initially when load is applied the stress is in proportion to strain i.e. material behaves elastically (Swab J. J., 2021) . After certain value the plastic flow starts, this means the strain happens more than the elastic limit. Once the elastic limit is achieved the material eventually fail in shear. Shear develops along a diagonal plane (Sines, 2013) . The fraction thus occurs due to bulging action, this is known as malleability. This property is associated with compression testing.

The requirement for the compression testing of the material is

- a. specimen must have larger cross-sectional area to resist any buckling due to bending
- b. specimen undergoing strain hardening as deformation proceeds,
- c. cross-section of the specimen increases with deformation

The buckling action causes instability, this can be avoided when the ratio of height to diameter of the specimen is less than 2. Thus lower the height to diameter ratio, higher is the compressive strength.

The procedure for the compression testing that was practiced was

- a. The sample of height to diameter ratio less than 2 was placed on the stage
- b. The stability of the sample was ensured
- c. Load was applied
- d. The trend of compression applied on the sample was initially linear
- e. At final stage sample was subjected to shearing due to load
- f. Load was removed
- g. From the graph plotted, values of compression were determined

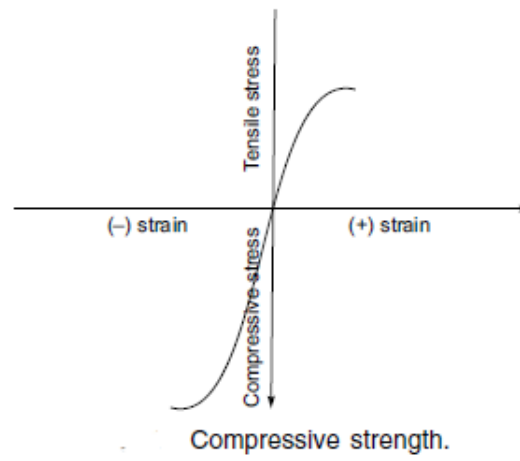


Fig.25 Graph representing stress/ strain curve during compression

Chapter 4

Results and Discussion

4.1 X-ray Diffraction (XRD)

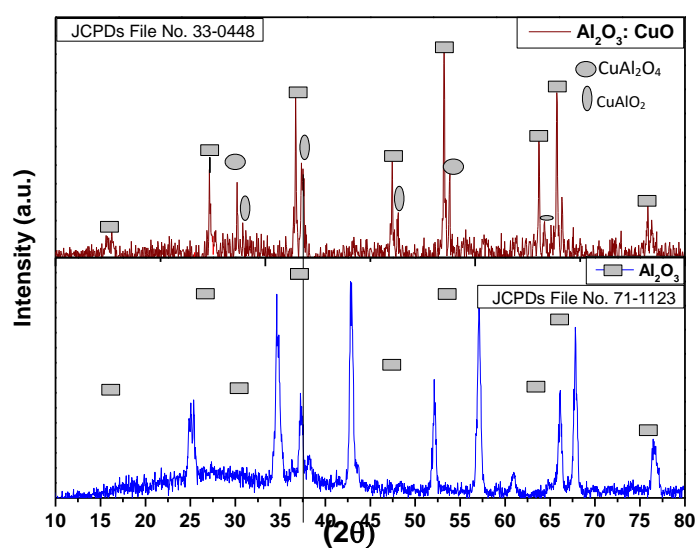


Fig.26 XRD comparison of Al_2O_3 and $\text{Al}_2\text{O}_3\text{-CuO}$

The graph stacked above represents the XRD patterns of pure alumina and alumina-copper oxide system, sintered at high temperature i.e. 1400°C , these are recorded in a wide range of Bragg angle 2θ i.e. from 5° to 80° . The lattice parameters calculated were close to, when compared with unit cell of alumina ($a = b = 4.761 \text{ \AA}$, $c = 12.87 \text{ \AA}$, JCPDs file No. 71-1123, to be $a = b = 4.781 \text{ \AA}$, $c = 12.98 \text{ \AA}$) (Prakash)

The slight peak shift and broadening of pure alumina peaks can be observed as the pellets were sintered at 1400°C .

The above graph represents the comparison of pure alumina and alumina with addition of copper oxide system. The weak peaks correspond to CuAl_2O_4 and a few traces of CuAlO_2 were identified. These peaks were quite prominent when higher concentration of copper oxide was added. The interaction of Cu-Al shows that the new phase was formed to promote liquid phase. The formation of these phase was started to be observed from 800 °C and above. (Fu, 2016)

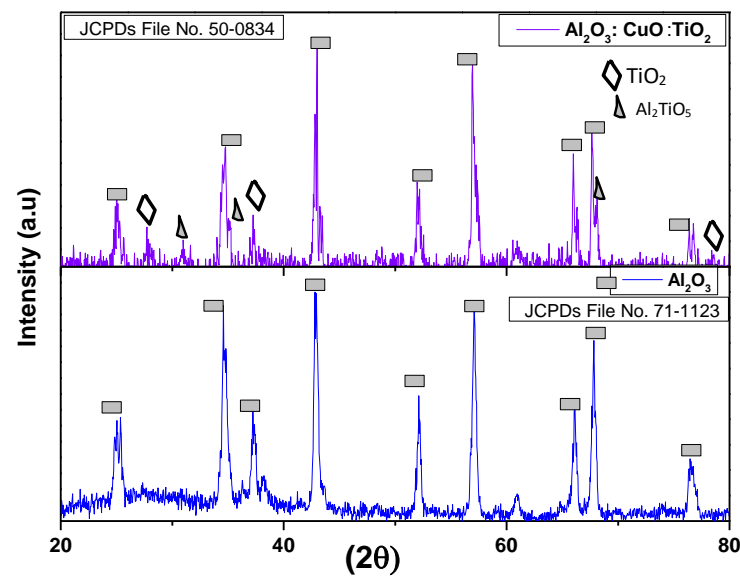


Fig.27 XRD comparison of Al_2O_3 and Al_2O_3 - CuO - TiO_2

In the alumina-copper oxide system when titania is added, the interaction of the three oxides can be proven by the help of the xrd graph, which demonstrates the presence of a new phase of titania with alumina along with those of copper oxide i.e. Al_2TiO_5 , CuAl_2O_4 and CuAlO_2 . When titania interacts with alumina it lowers its sintering activation energy. This not only enhances the atomic diffusion but also helps in promoting sintering as increases the lattice defects. When these phases are formed and the interaction of copper oxide and titania at a eutectic temperature where melt is formed causes the formation of distortion and vacancy. These play a vital role for alumina to recrystallize and densify effectively (Clarke, 1989).

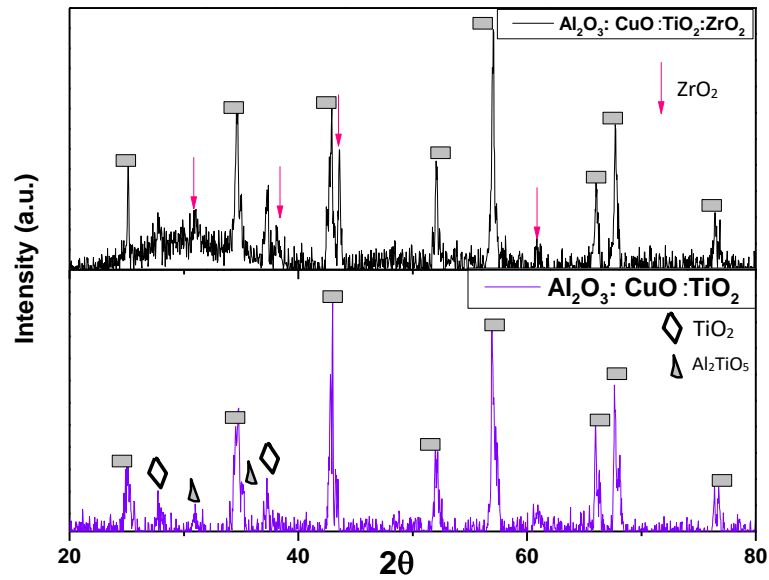


Fig.28 XRD comparison of $\text{Al}_2\text{O}_3\text{-CuO-TiO}_2$ and $\text{Al}_2\text{O}_3\text{-CuO-TiO}_2\text{-ZrO}_2$

The graph is a comparison between the alumina system (copper oxide and titania) with and without the addition of ZrO_2 . The ZrO_2 is present in its monoclinic phase and a tetragonal phase can also be observed. In the composition where ZrO_2 added up to 1 wt% the monoclinic phase was prominent but as the content of ZrO_2 increased the tetragonal phase of ZrO_2 can be observed in the graph. From various sources it has been proven that the monoclinic phase is responsible for the strength, when interacts with the alumina but in our study, this is not the case. Another, effect can be observed that tetragonal phase of zirconia increases than usual due to the presence of TiO_2 . (Hossen M. M., 2014)

4.2 Scanning Electron Microscopy (SEM)

4.2.1 Addition of CuO

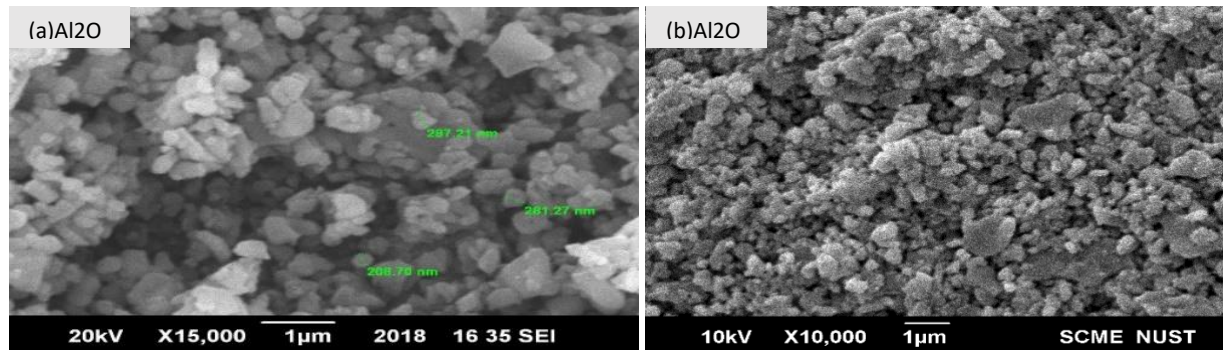


Fig. 29 SEM image of pure alumina at (a) 1300°C, (b) 1400°C

The above fig.29 represents the sem image of pure alumina compact, sintered at 1300°C and 1400°C, respectively. The images show that particles subjected to high temperature might have formed clusters, but no other significant effect can be observed. The formation of clusters can be due to the pressure exerted during pallet formation. The size of the particles remained to be between 0.2µm to 0.4µm. Hence, the temperature had no effect on the alumina compaction and density is not affected.

The addition of CuO in alumina as a sintering additive was carried out. The weight percentage considered was 1wt%, 3wt%, 5wt%, and 8wt%. The pallets were formed under 2-ton pressure for 3 min. These green compacts were then sintered at 1300°C and 1400°C.

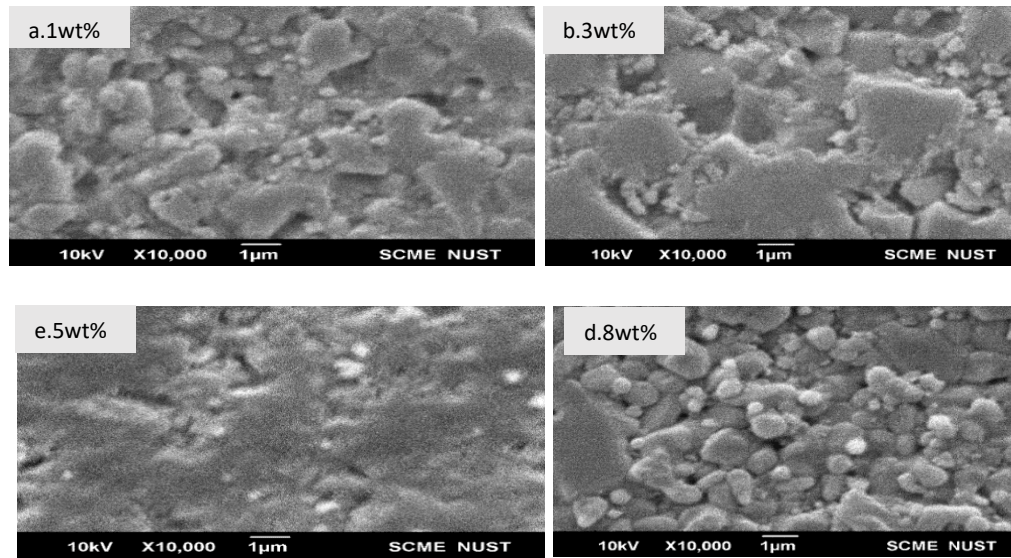


Fig.30 SEM images of at 1300C (a) Al₂O₃- 1wt% CuO, (b) Al₂O₃- 3wt% CuO, (c) Al₂O₃- 5wt% CuO, and (d) Al₂O₃- 8wt% CuO

The sem images were taken of the alumina compact sintered at 1300C. The fig.30(a) shows the effect of addition of 1wt% CuO in alumina. The pellet when subjected to high temperature it undergoes phase formation i.e., CuAl₂O₄ is formed, which is the cause of liquid phase sintering. The melting point of alumina is 2070C needed to densify alumina in conventional manner, thus, to achieve liquid phase sintering is an important step as it helps in compaction of alumina, at low temperature. The liquid phase CuAl₂O₄, formation in between the grain boundaries of alumina particles gives of continuous plain areas which shows that diffusion has occurred thus capillary forces are in effect. But due to low concentration of CuO the coverage throughout the sample, of liquid phase is limited hence patches of continuous plain surfaces were obtained.

In the fig.30 (b) and (c) the concentration of CuO was increased to 3wt% and 5wt% respectively. A positive trend of the increase of sintering additive could be observed in the above given images. The liquid phase CuAl₂O₄, formed throughout the sample giving of larger regions of continuous surfaces results in improved compaction.

Further study shows that increase of sintering additive i.e., CuO up to 8wt% has not resulted to be positive but porosity has increased, this can be explained that a high amount of CuAl₂O₄ restrains

grain growth or another case occurring is CuO instead of forming a new phase has undergone solid state reaction with Al₂O₃ forming larger or diffused elongated like shapes (Fu, 2016).

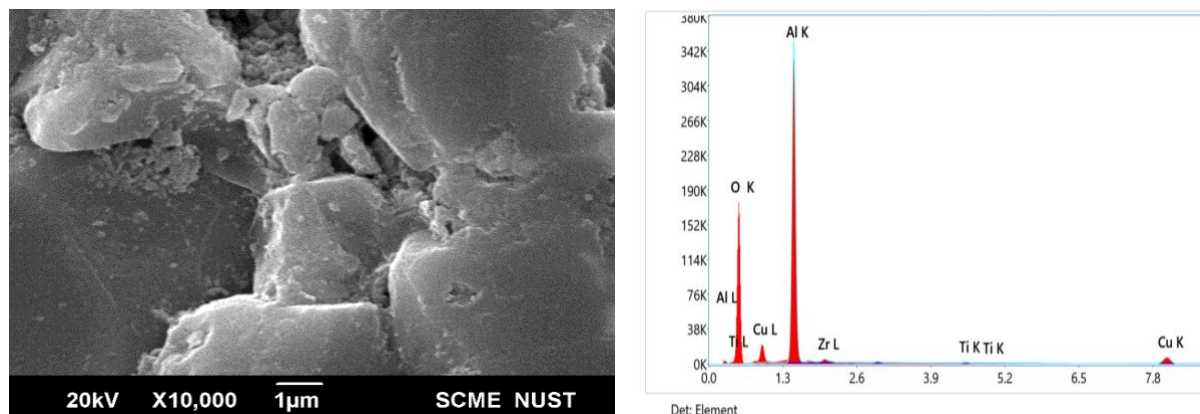


Fig 31 SEM image of 5wt% CuO at 1400C and EDS

Table 5. EDS weight ratio focused on specific area

Sample	Temperature	Aluminum		Copper		Oxygen	
		Wt%	At%	Wt%	At%	Wt%	At%
1	1300C	58.5	45.8	2.9	1	38.4	53.2
2	1400C	78	89.4	20	9.7	35.7	45.8

From the previous sem results it was evident that sample of alumina containing 5wt% CuO gives of maximum continuous region due to presence of optimum liquid phase thus a better coverage and compaction throughout the alumina sample was obtained. hence the further studies made were concentrated on this specific concentration, i.e, 5wt% of CuO. The above fig31 represents the sem image of alumina containing 5wt% CuO, which was sintered at 1400C. The EDS taken was to confirm the elemental detections and the homogeneity obtained throughout the region. The region observed in SEM image exhibits that a diffusion has occurred and liquid phase present between the alumina-alumina grain boundary provided continuous smooth areas. The alumina sample sintered at 1400C gave much better result than that sintered at 1300C, which is evident from the micro-structure given above.

4.2.2 Addition of CuO: TiO₂ in Al₂O₃

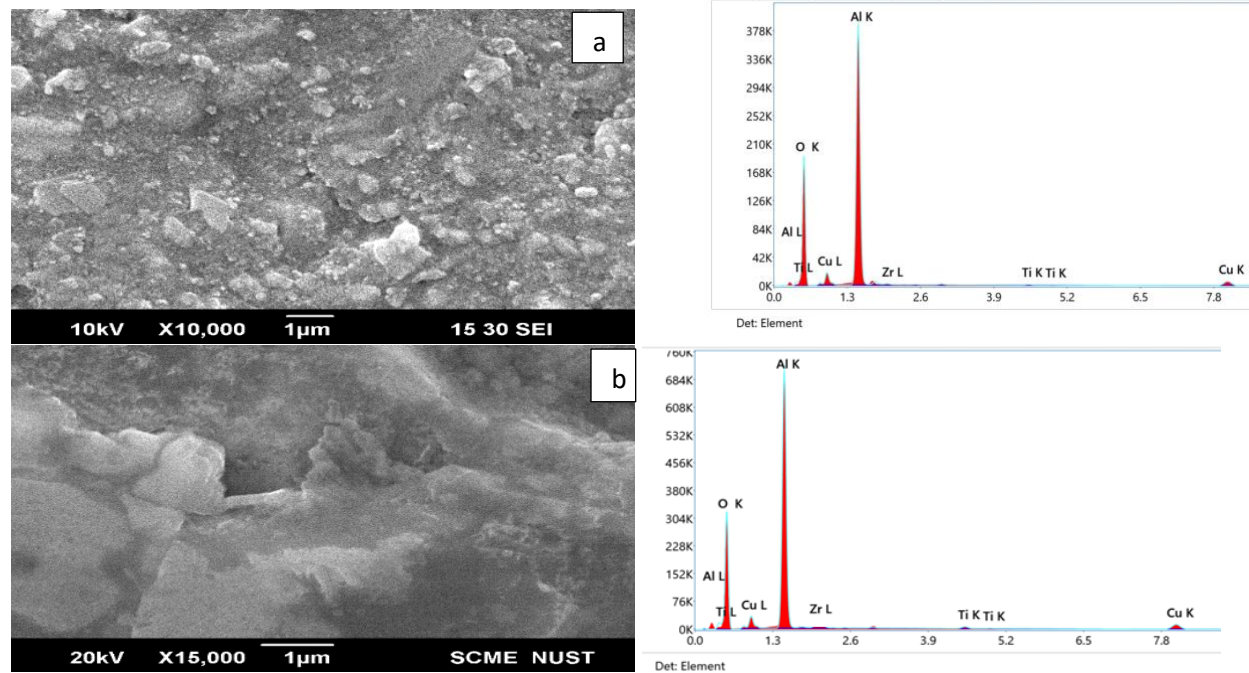


Fig. 32 SEM image of Al₂O₃- 5wt% CuO- TiO₂ at a)1300⁰C and b)1400⁰C

Table 6. EDS weight ratio focused on specific area

Sample	Temperature	Aluminium		Copper		Titanium		Oxygen	
		Wt%	At%	Wt%	At%	Wt%	At%	Wt%	At%
1	1300 ⁰ C	48.3	38.1	6.3	2.1	0.8	0.1	45.4	59.6
2	1400 ⁰ C	45.8	37.3	7.5	3.2	0.8	0.4	44	59.1

The compaction of Al₂O₃ system when CuO was added gave favorable results, the next step was to observe if along with liquid phase solid phase could be introduced to enhance the morphology needed to ensure compaction of alumina pellets. Thus, it was required to produce vacancies in the lattice of alumina, thus TiO₂ was considered and was added in 2wt% concentration along with CuO

(1wt%,3wt%,5wt%,8wt%). The best results obtained were of 5wt% of CuO added in Al₂O₃-CuO-TiO₂ system, which was discussed here. The fig 32 (a), (b) represents the sem images of the samples sintered at 1300⁰C and 1400⁰C, respectively, along with EDS that represents the elemental configuration and the homogeneity of the additives throughout the sample. Sample sintered at 1300⁰C, it was observed that there is a continuous phase throughout the sample. The densification behavior depends on the associations of pores with grain growth and the mode of grain growth. Since the phases CuAl₂O₄ and AlTiO₂ were formed; the di-phases occurred due to the mass transfer and diffusion phenomena. This gave rise to the flattening at the point of contact thus decreasing the angularity of grains. The capillary effect can be observed when liquid phase surrounds the alumina-alumina grains, decreasing the porosity. While TiO₂ creates vacancies in Al₂O₃ lattice forms a solid phase as both have tetragonal structures (Clarke, 1989). The densification and a solid-state reaction occur at approximately 1300⁰C. This gives higher compaction of the alumina as can be observed from the fig.32(a). The SEM image of the sample sintered at 1400⁰C shows a better distribution of liquid phase throughout. Additional densification was achieved as the rearrangement of particles became insignificant. The mechanism followed was, dissolved solute transferred to the parts of grain structure by diffusion followed by reprecipitation.

4.2.3 Addition of CuO: TiO₂: ZrO₂

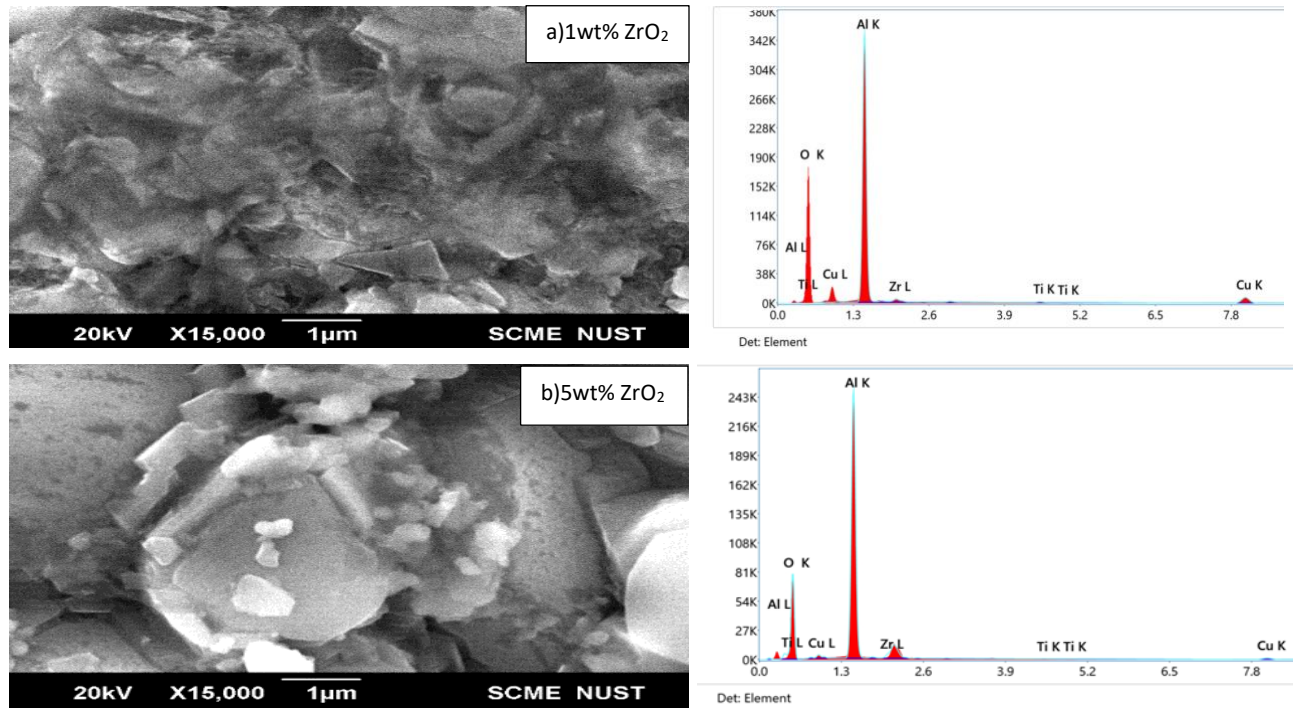


Fig 33. SEM images of a) Al₂O₃-CuO-TiO₂-1 wt%ZrO₂ and b)Al₂O₃-CuO-TiO₂-5wt%ZrO₂ at 1300 °C

Table 7. EDS weight ratio focused on the specific area

Sample	Temperature	Wt% of ZrO	Aluminum		Copper		Titanium		Zirconia		Oxygen	
			Wt%	At%	Wt%	At%	Wt%	At%	Wt%	At%	Wt%	At%
1	1300°C	1wt%	70	88.5	16.4	7.9	0.7	0.4	2.9	0.13	10	12.2
2		5wt%	68.1	83.4	13.4	9.7	0.7	0.5	1.2	0.4	16.6	6

ZrO₂ has been used to increase the mechanical strength of pure alumina and is used in various applications mostly biomedical-based, our purpose was to conclude a system that can increase densification and induce better mechanical results. A multi-phase, alumina system was introduced by

adding ZrO_2 along with CuO and TiO_2 , which were sintered at $1300\text{ }^{\circ}C$ and $1400\text{ }^{\circ}C$. The ZrO_2 added were 1wt% and 5wt%. The diphasic and multi-phasic effect combined is observed.

The sem images (a) (b) shown in the above fig.33 represent that as ZrO_2 added in 1wt% and 5wt% respectively and were sintered at $1300\text{ }^{\circ}C$. In the multiphase system of alumina the ZrO_2 added in lower concentration i.e, 1wt% has changed the morphology but yet has no significant effect on the structure observed in fig.33(a) but as the concentration was increased to 5wt% of ZrO_2 it is quite evident that the surface is no longer continuous which can be observed from the sem image fig.33 (b). It was observed that grain size varies as the amount of ZrO_2 was added to the Al_2O_3 system. The continuous phase present in various areas of the compact surface was due to the presence of CuO and TiO_2 , while the coarsening is due to the partial oxidation of ZrO_2 . The ZrO_2 reacts with Al_2O_3 to form a solid state reaction (Hossen M. M., 2014). The porosity and cracks can be observed as could be seen between the small regions of abnormal grain growth areas evident in fig 33 (b).

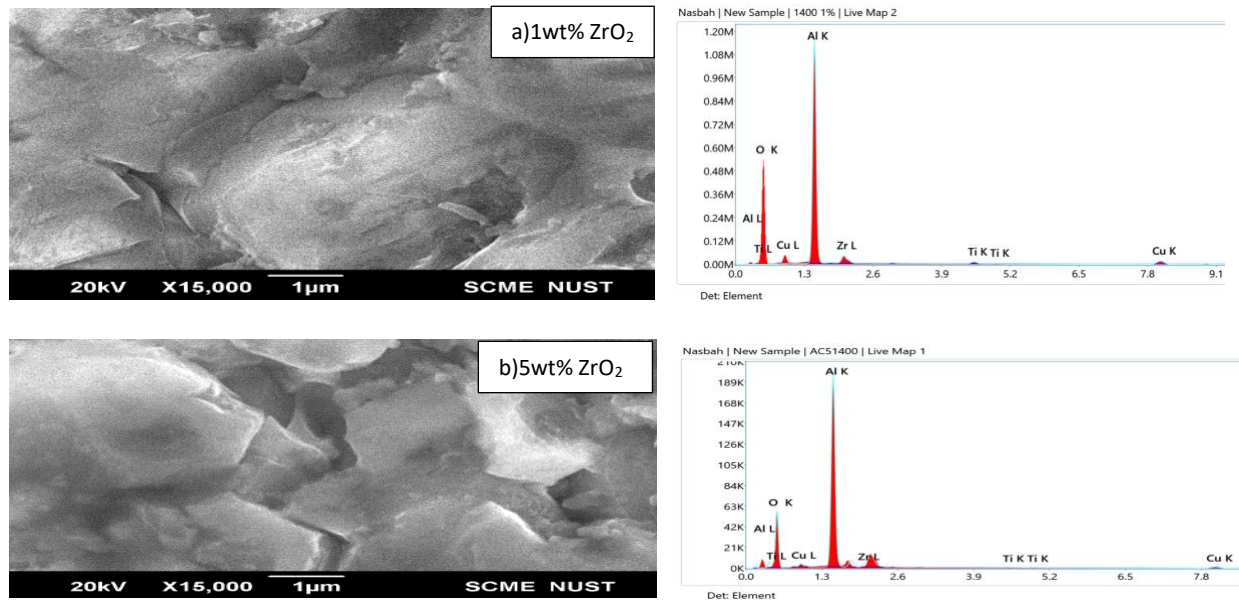


Fig 34 SEM images of a) $sAl_2O_3-CuO-TiO_2-1\text{ wt}\%ZrO_2$ and b) $Al_2O_3-CuO-TiO_2-ZrO_2$ at $1400\text{ }^{\circ}C$

The sem images (a) (b) shown in the above fig.34 represent that as ZrO_2 added in 1wt% and 5wt% respectively and were sintered at $1400\text{ }^{\circ}C$. In this multiphase system of alumina the ZrO_2 added in lower concentration i.e, 1wt% has affected the morphology as could be observed in fig.34(a). The same

effect was observed when the concentration was increased to 5wt% of ZrO₂ as it was quite evident from the surface in sem image fig.34 (b). The continuous phase present in various areas of the compact surface was due to the presence of CuO and TiO₂, while the coarsening is due to the partial oxidation of ZrO₂. The ZrO₂ reacts with Al₂O₃ to form a solid state reaction (Hossen M. M., 2014). From the given fig.34(b) high porosity and cracks can be observed between the small regions of abnormal grain growth regions.

Table 8. EDS weight ratio focused on the specific area

Sample	Temperature	Wt% of ZrO	Aluminum		Copper		Titanium		Zirconia		Oxygen	
			Wt%	At%	Wt%	At%	Wt%	At%	Wt%	At%	Wt%	At%
1	1400°C	1wt%	70.4	80	10.8	5.3	1.9	1.2	7	2.2	14	11.3
2		5wt%	45.8	37.3	6.5	2.3	0.8	0.4	3	0.9	43	59.1

4.3 Density

Once pellets were sintered, the densification was calculated. The pellets of the three systems of alumina was prepared at 1300°C and 1400°C, respectively. Considering the alumina system in which

CuO was added, its densification was plotted against pure alumina at 1300°C and 1400°C.

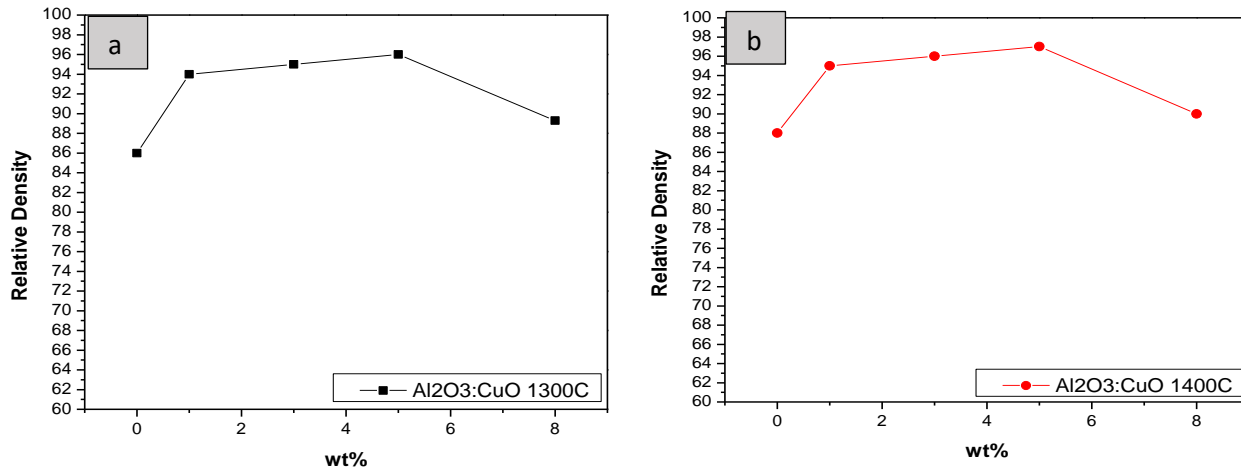


Fig.35 Relative density graph of pure alumina and Al₂O₃-CuO system at (a)1300°C and (b)1400°C

The above graph shows that pure alumina's relative density is less than that of alumina containing CuO(1wt%,3wt%,5wt%,8wt%). This result could be supported by the sem images obtained in fig.30 and fig31 respectively. The densification obtained shows an increasing trend as the concentration of CuO increases. But this trend can be observed till the concentration reaches 5wt% of CuO. This can be explained based on liquid phase formation, wettability, and diffusion throughout the microstructure.

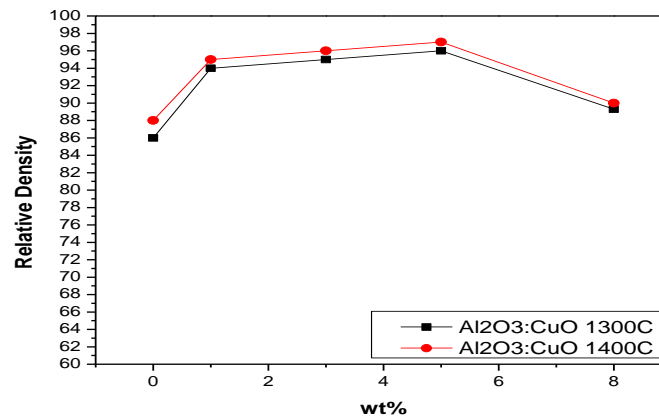


Fig.36 Comparison of Relative density graph of pure alumina and Al₂O₃-CuO system at (a)1300°C and (b)1400°C

The trend is shown in fig.36 where a comparison was made, that temperature increase has a positive effect on the densification of the alumina system, and with these concentrations of CuO, the 5wt% has shown good results in comparison to the others. But as the concentration increased to 8wt% despite the temperature provided densification decreased.

Considering the di-phase alumina system i.e CuO-TiO₂ is added as sintering additives.

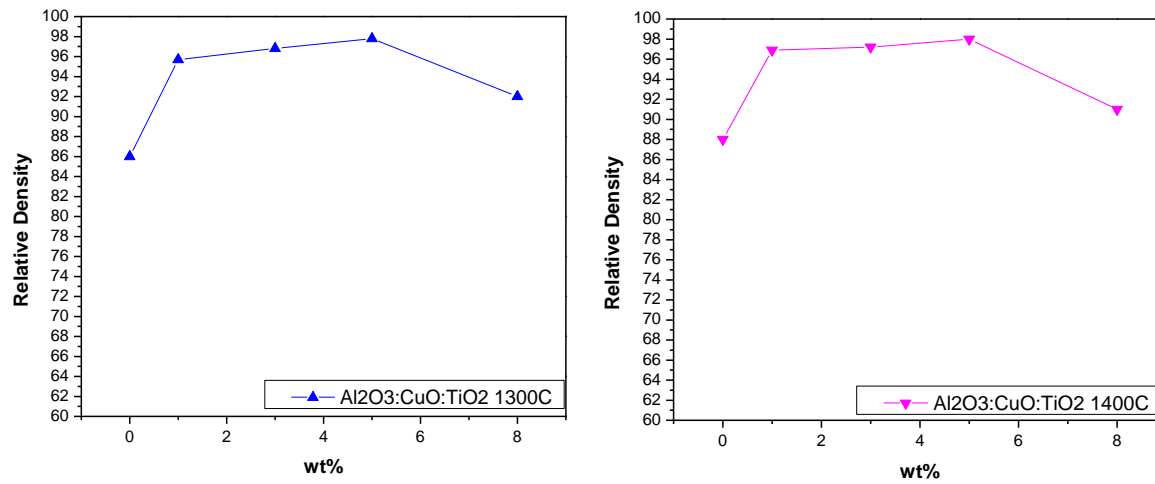


Fig.37 Relative density graph of pure alumina and Al₂O₃-CuO- TiO₂ system at (a)1300°C and (b)1400°C

The above fig.37 shows the relative density increasing trend till the 5wt% concentration of CuO, but exceeding this optimum concentration showed that density falls drastically. Thus the most favorable result achieved in the di-phase alumina system was at 5wt%. The doping effect of TiO₂ seemed to favor pore elimination resulting in high densification of the alumina sample.

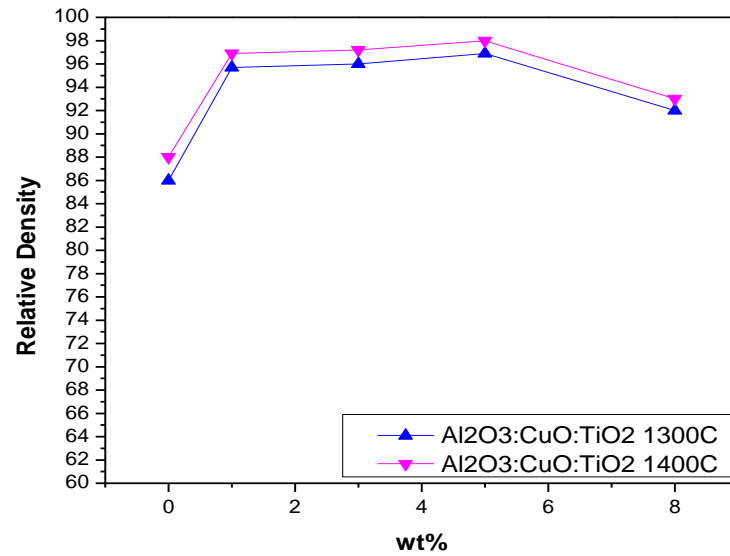


Fig.38 Relative density graph of pure alumina and Al₂O₃-CuO-TiO₂ system at (a)1300°C and (b)1400°C

The above figure gives a comparative study of the alumina system when CuO-TiO₂ was added and sintered at 1300°C and 1400°C. The graphs show that as temperature increases it gives off more refined compaction thus resulting in higher densification at 1400°C than at 1300°C.

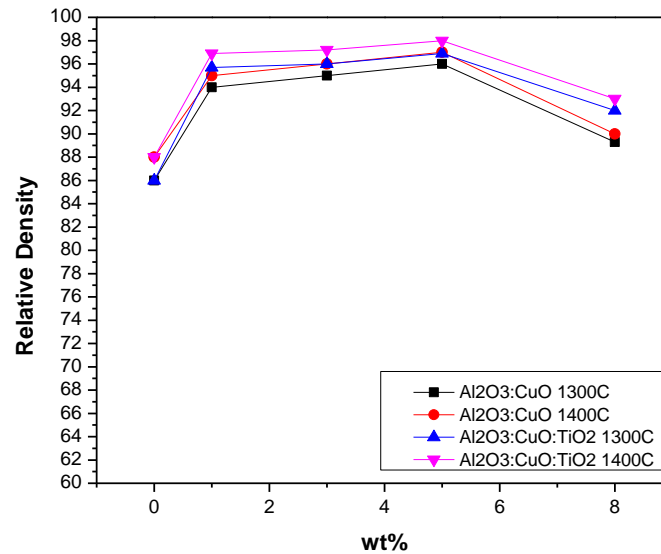


Fig. 39 Relative density comparison of Al₂O₃-CuO and Al₂O₃-CuO-TiO₂ system

The above graph draws a comparison of the single-phase alumina system and di-phase alumina system. With the increase in Concentration of CuO up to an optimum concentration value i.e., 5wt% the trend seemed to be of increasing order, but further increase in CuO concentration in both systems causes degradation in the values of densification. This can be explained that the liquid phase formed in a higher quantity produces the coarsening effect, thus it induced distortion and deformation of the surface, causing a decrease in densification. Similarly, with the increase in temperature, the density of the specimens also increases. The increase in temperature supports vibrational motion and diffusivity of the liquid phase. The diffusivity of the liquid phase is high as most of the CuO present in the alumina matrix reacts to form new phases, while TiO₂ also forms a new phase with Al₂O₃ i.e. Al₂TiO₂ thus promoting fast grain growth due to reprecipitation phenomena. (HaiyangLi, Low-temperature sintering of coarse alumina powder compact with sufficient mechanical strength, 2017)

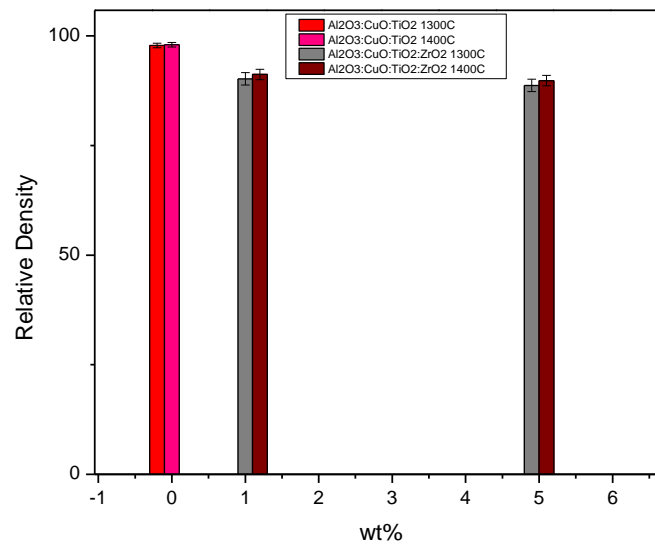


Fig 40. Density comparison of Al₂O₃-CuO-TiO₂ and Al₂O₃-CuO-TiO₂- (1,5 wt%) ZrO₂

From previous data, a conclusion can be drawn that the CuO 5wt% concentration has the desirable result of densification. Thus, this concentration was further used in a series of experiments when considering a multi-phase system i.e Al₂O₃: CuO(5wt%): TiO₂: ZrO₂ (1,5 wt%) system. According to the above graph, the trend of densification shows that as temperature increases the densification also increases. When the increase in the concentration of ZrO₂ was considered in the multi-phase system it resulted in an adverse effect on the alumina. A comparison of di-phase and multi-phase was established that showed that di-phase densification is better than multi-phase densification.

4.3 Micro-Vickers Hardness

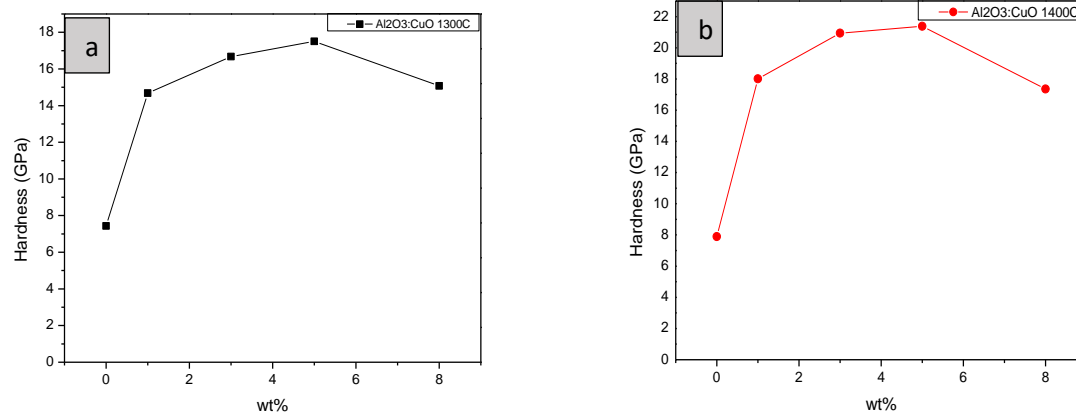


Fig.41 Vickers Hardness of pure alumina and Al₂O₃-CuO system at (a)1300°C and (b)1400°C

Hardness is the measure of resistance to localized deformation of a material. From the above graph given in fig40. (a) and (b) hardness of Al₂O₃-CuO system is shown at 1300°C and 1400°C, respectively. The trend above shows that hardness increased when CuO was introduced, as compared to the pure alumina. It can be seen that as concentration of CuO was increased upto 5wt%, the increase in hardness can be observed, but as the concentration increased to 8wt% a decrease in hardness was seen. Thus the most favorable results were shown by sample containing 5wt% CuO in alumina system at both temperatures i.e, 1300°C and 1400°C. Thus at the sintering temperatures the liquid phase has aided in enhancing hardness of alumina even at such low temperatures.

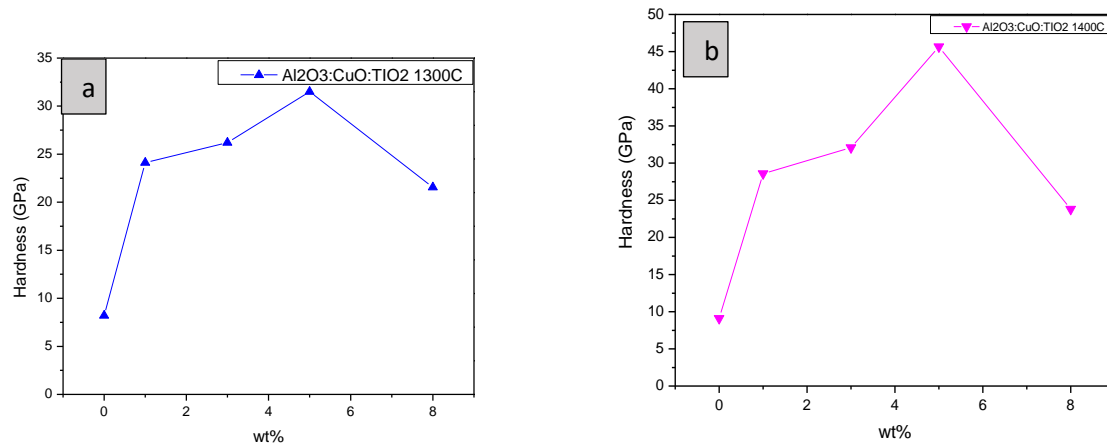


Fig.42 Vickers Hardness graph of pure alumina and Al₂O₃-CuO- TiO₂ system at (a)1300°C and (b)1400°C

From the above graph given in fig40. (a) and (b) hardness of Al₂O₃-CuO-TiO₂ system is shown at 1300°C and 1400°C, respectively. The trend above gives more favorable results of hardness as increasing trend could be observed when CuO and TiO₂ was introduced, as compared to the result shown by pure alumina. It can be seen that as concentration of CuO was increased up to 5wt%, the increase in hardness can be observed, the di-phase causing the formation of CuAl₂O₄ and AlTiO₂ aided in achieving increased value of hardness. The further increase in the concentration up to 8wt% gave diverse effect i.e., a decrease in hardness value was seen. Thus the most favorable results were shown by sample containing 5wt% CuO- TiO₂ in alumina system at both temperatures i.e, 1300°C and 1400°C.

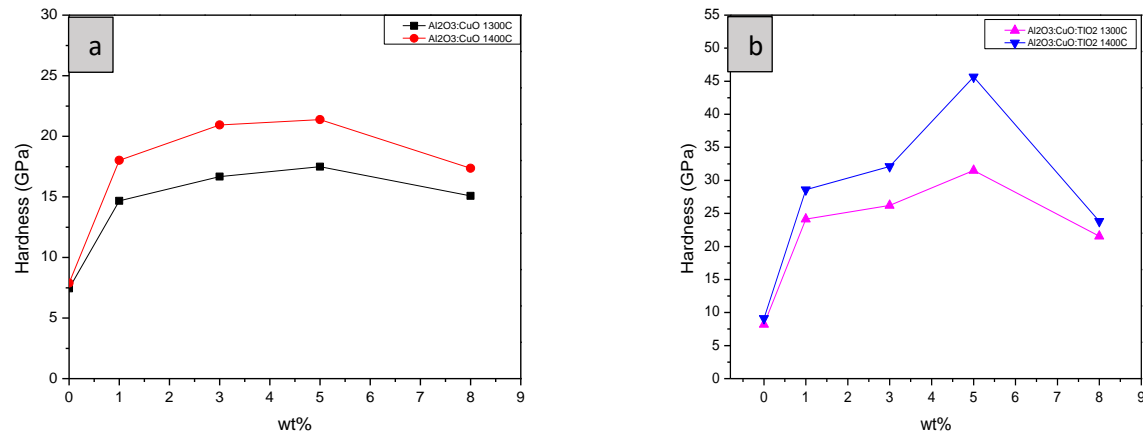


Fig. 43 Vickers Hardness values of (a) Al₂O₃-CuO and (b) Al₂O₃-CuO-TiO₂ at 1300°C and 1400°C

Hardness is directly proportional to the densification of the material. The trend of hardness from the above graphs justifies the results of relative density discussed in the section 4.2. Observing the fig.42 (a) and (b) gives a comparison of sintering temperature of Al₂O₃-CuO system and Al₂O₃-CuO-TiO₂ system, respectively. The trend in both cases represents that as the temperature increases, values of hardness also increases which is evident from the graphs above. It can be said that hardness is temperature dependent. The solubility of Cu ion in alumina explained through phase diagram in **fig.14**, shows that CuAlO₂ forms a liquid phase below 1000°C. This phase helps in diffusion as it has wettability property while Al₂TiO₅ formed during solid phase sintering helps in increase of hardness. However when the concentration of CuO was increased to 8wt% the adverse effect can be observed, the hardness decreased which was due to presence of higher concentrations of copper oxide where the phase appears in metastable state thus decompose easily, producing the porosity.

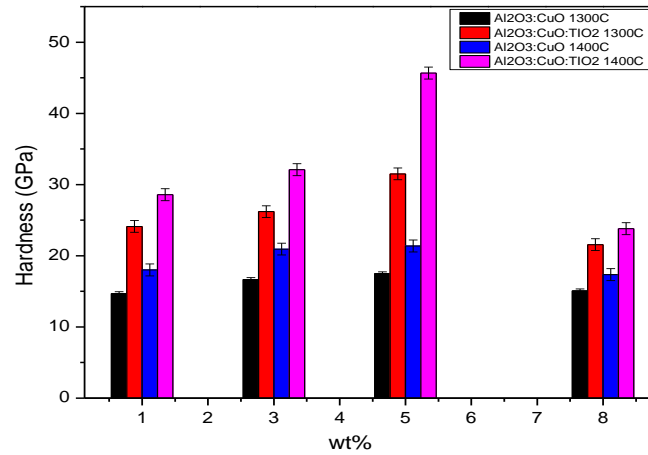


Fig. 44 Vickers Hardness values comparative study of Al₂O₃-CuO and Al₂O₃-CuO-TiO₂

The figures above represents hardness of the two system i.e (a)Al₂O₃: CuO and (b)Al₂O₃: CuO: TiO₂ system and a comparative study in fig35 (c) has been made. The hardness is directly proportional to the densification of the material. Increasing the sintering temperature increased hardness. The two systems when compared shows the system containing di-phase i.e., CuO and TiO₂ gave much favourable results than that alumina system containing single phase i.e.,CuO. This is due to the fact that the di-phases formed i.e., CuAlO₂, Al₂TiO₅ were formed, which has aided the alumina system.

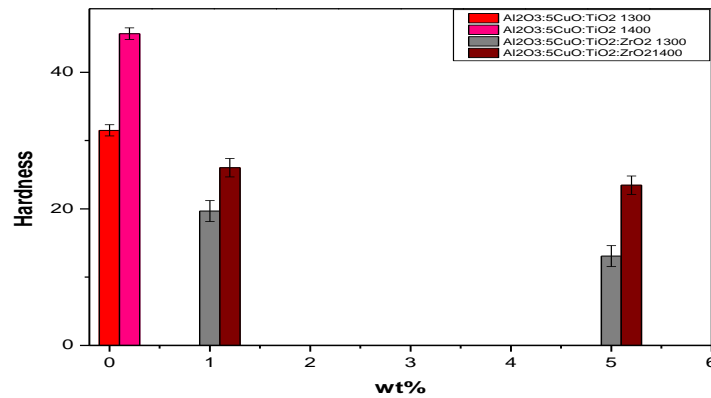


Fig. 45 Vickers Hardness values comparison of Al₂O₃-CuO-TiO₂ and Al₂O₃-CuO-TiO₂-(1-5 wt%) ZrO₂

From previous data a conclusion can be drawn that the CuO 5wt% concentration in both single phase, and di-phase alumina system has shown desirable result . This concentration was further used in series of experiments when considering a new multi-phase system i.e Al₂O₃: CuO(5wt%): TiO₂: ZrO₂ (1,5 wt%) system. The fig.44 shows a comparative study of hardness of the two system i.e. diphase- and multi-phase system. The addition of ZrO₂ in a multi-phase alumina decreased hardness values as compared to the hardness values of di-phase system. [61]

4.4 Universal Testing Machine

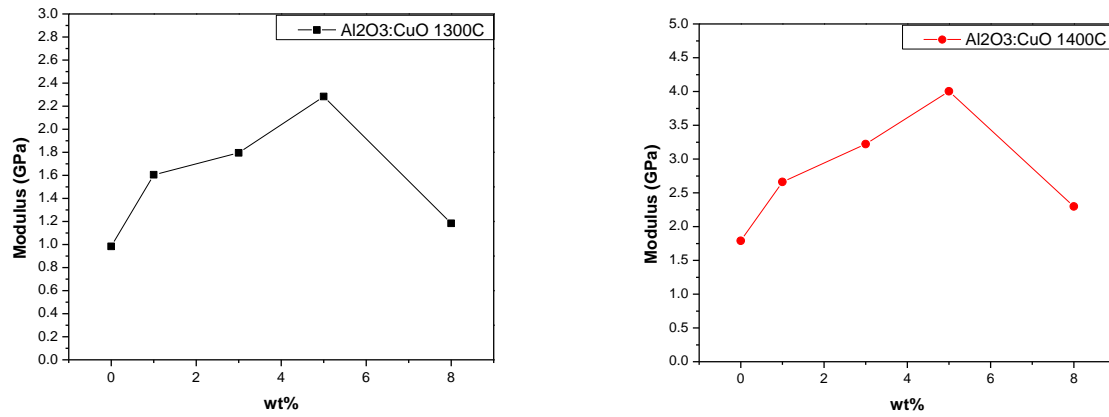


Fig.46 Compression testing graph of pure alumina and Al₂O₃-CuO system at (a)1300°C and (b)1400°C

Compression testing is the study of the material to withstand crushing force when load is applied. The fig.45 above represents compression testing of the alumina system i.e., Al₂O₃-CuO system at (a) 1300°C and (b)1400°C. The graph exhibits the increasing trend i.e., compression strength of alumina system increases as compared to that of pure alumina. From the above result it could be established that as density of the alumina samples, increases, value of compression also improves. This trend was observed till the concentration of CuO was up to 5wt% but as the concentration of CuO increases to 8wt% the compression value decreases drastically, at both temperature conditions i.e, 1300C and 1400C respectively. This is due to the fact that higher values of CuO in alumina restrains grains growth which decreases the densification due to formation of irregularities within the sample structure, thus porosity is introduced and hence cause initiation of microcracking even at a very minimum load.

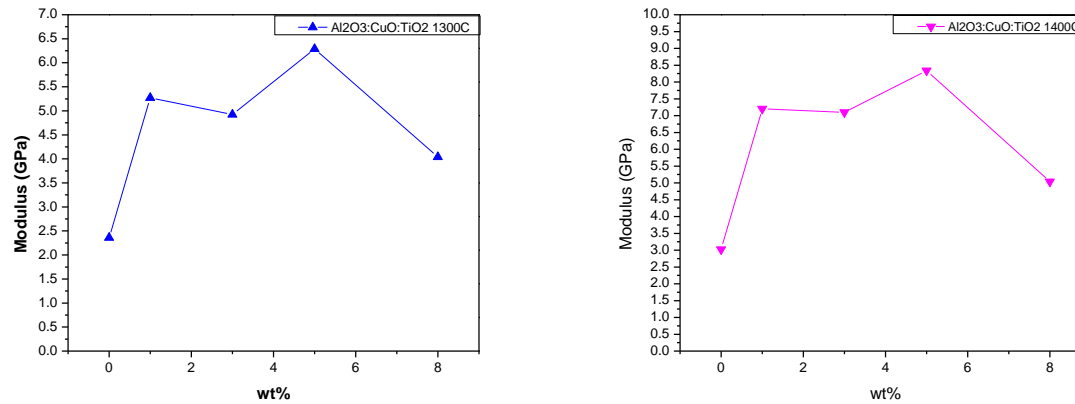


Fig.47 Compression testing graph of pure alumina and $\text{Al}_2\text{O}_3\text{-CuO-TiO}_2$ system at (a)1300°C and (b)1400°C

The fig.45 above represents compression testing of the alumina system i.e., $\text{Al}_2\text{O}_3\text{-CuO-TiO}_2$ system at (a) 1300°C and (b)1400°C. The compression values increased as sintering additives were added up to 5wt% concentration. The di-phase present in the alumina system due to the presence of liquid phase acting as binder while titania undergoes solid phase sintering. The values improved in this system as compared to that of the pure alumina. Concentration when increased to 8wt% a drastic fall in the values could be observed from the above graph given in fig.46 because the higher concentrations caused restriction of grain growth and porosity was introduced.

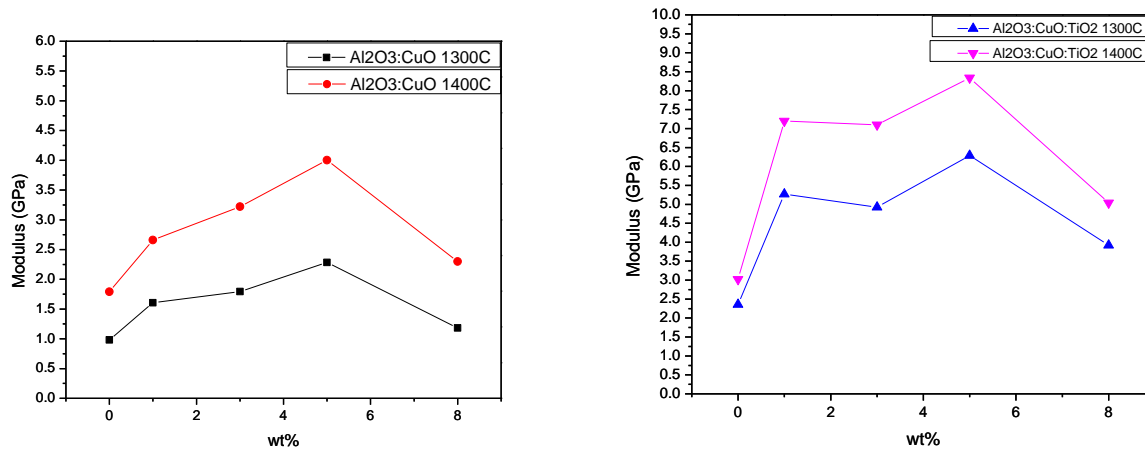


Fig. 48 Compression testing graph of (a) Al₂O₃-CuO and (b) Al₂O₃-CuO-TiO₂ at 1300°C and 1400°C

Compression is also temperature dependent. A comparison of both systems i.e, (a) Al₂O₃-CuO and (b) Al₂O₃-CuO-TiO₂ **comparison** is given on the basis of temperature. At 1300°C the values of compression are lower than those samples sintered at 1400°C in both systems. This can be observed in above fig.47 provided. As the sintering temperature of samples increased the compression strength of these samples also increased, this is due to the fact that at higher temperatures the compaction of these samples was higher as liquid phase present acted as a binder thus density increased. This means that the phases formed during sintering has promoted grain growth and penetration through grain boundaries covering the particles thus provided maximum strength to the system under optimum concentration of CuO, in both the systems. But despite the higher temperatures provided, from the fig.47 (a) and (b) compression increased up to 5wt% CuO added, but further increase in concentration of CuO to 8wt% porosity was introduced hence causing microcracking even at a very minimum load, the decrease in compression strength value was clear, in both systems above.

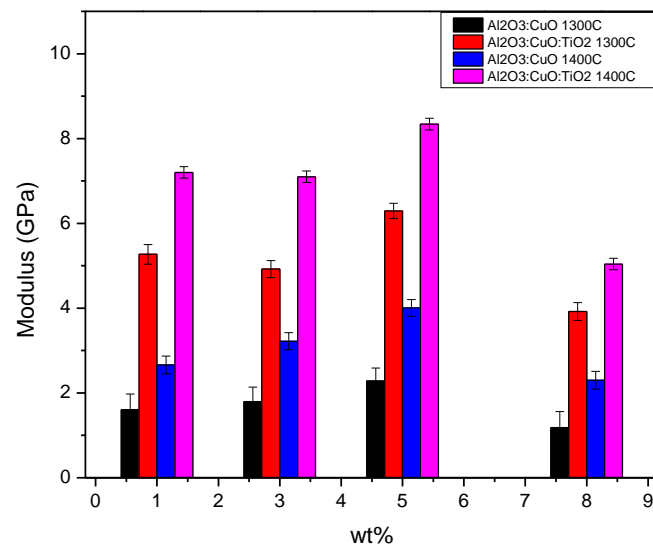


Fig.49 Comparative study of ompression testing values of (a)Al₂O₃-CuO and (b)Al₂O₃-CuO-TiO₂

The above graphs gives a comparative demonstration of both the systems at given temperatures i.e, 1300C and 1400C at diffrenet concentrations of CuO (1wt%, 3wt%, 5wt% and 8wt%)

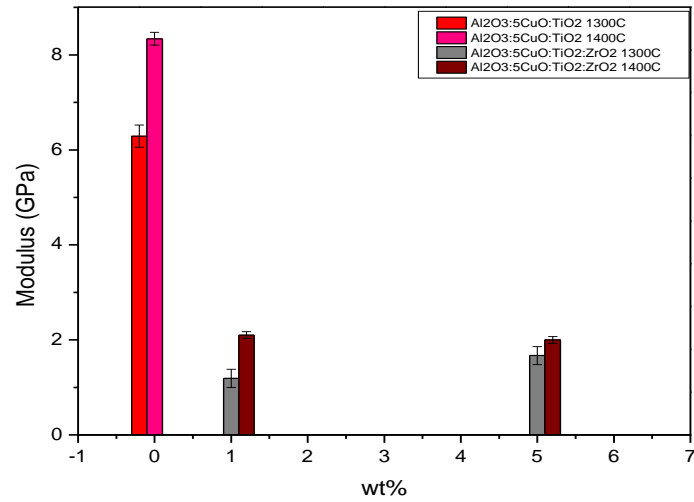


Fig.50 Compression testing values comparison of Al₂O₃-CuO-TiO₂ and Al₂O₃-CuO-TiO₂- (1-5 wt%) ZrO₂

From previous data a conclusion can be drawn that the CuO 5wt% concentration has shown desirable result . This concentration was further used in series of experiments when considering a multi phase system i.e Al₂O₃: CuO(5wt%): TiO₂: ZrO₂ (1,5 wt%) system. The comparison of the two systems, di-phase (CuO(5wt%): TiO₂) and multi-phase [CuO(5wt%): TiO₂: ZrO₂ (1,5 wt%)] in alumina matrix has been established. The multi-phase system simply shows a drastic decrease in compression values when ZrO₂ was introduced. This can be explained that the coarsening effect of ZrO₂ grains inducing porosity, thus, causing microcracking and its propogation at a very low value of load thus the specimen could not withstand even a slightes load.

Conclusion

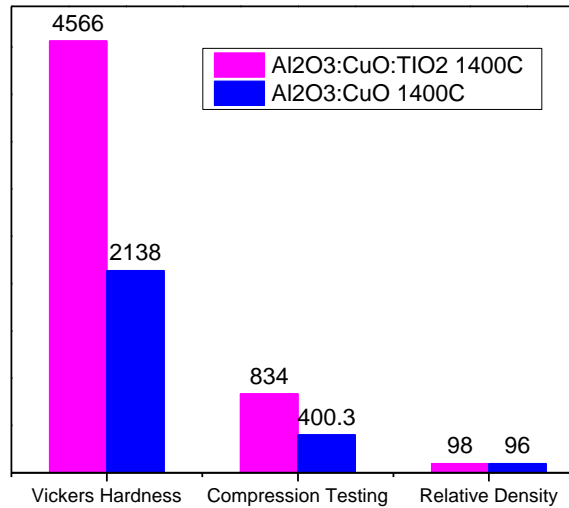


Fig.51 Represents values of 5wt% CuO added in Al₂O₃-CuO and Al₂O₃-CuO-TiO₂ system at 1400°C

From the above results it can be deduced that the densification of alumina is possible and increases when copper oxide was initially added. The effect of hardness and compression of these samples when tested, which gave an increasing trend till 5wt% concentration of CuO in alumina matrix. This was the optimum concentration because as CuO concentration was further increased to 8wt% the results drastically decreased.

In di-phase alumina system addition of CuO and TiO₂ when added in an optimized concentration i.e 5wt% of CuO. This also gave the increase in density of alumina system and increase in mechanical properties. CuO forming liquid phase between the alumina-alumina grain boundaries, increased the interfacial strength. While the addition of TiO₂ causes creates vacancies in alumina lattice, thus undergoing solid state reaction. This aided in further decrease in internal porosity as densification was increased. The combination of the two prompts the grain size.

However, when forming a multi-phased alumina system, the addition of ZrO_2 along with CuO and TiO_2 was made. The addition of low concentration of ZrO_2 i.e., 1 wt% has no significant effect on the morphology of alumina system but has drastically decreased the mechanical properties of the system. Secondly, when the ZrO_2 concentration was increased to 5wt% it has affected the morphology of alumina system as cracks and porosity could be observed. When these samples tested, they exhibited decrease in the values of densification and mechanical properties. Thus, an optimized concentration needs to be obtained for better results and at various temperatures this system needs to be studied.

References

1. *T.Khalil. (2000). Preparation, Characterization and application of Alumina powder. *Seventh Conference of Nuclear Sciences & Applications*. Cairo.
2. B, J. (2009). *Mechanical Properties of Ceramics, Second Edition*. John Wiley & Sons, Inc.
3. BARMORE, W. L. (1965). High-Temperature Plastic Deformation of Polycrystalline Beryllium Oxide. *Journal of the American Ceramic Society*, 48(10), 499-505.
4. Bishui, B. M. (2014). Thermal Conductivity of Ceramic Materials. *Transactions of the Indian Ceramic Society*, 17(3), 8-116.
5. Boldin, M. S. (2022). Investigation of the Densification Behavior of Alumina during. *Materials*, 15, 2167.
6. Botinelli, A. (1988). Densification of alumina at 1400 0C. *Ceramics International*, 14, 31-34.
7. Bunaciu, A. A. (2015). X-Ray Diffraction: Instrumentation and Applications. *Critical Reviews in Analytical Chemistry*, 45(4).
8. Burke, J. E. (1976). Sintering. In *Treatise on Solid State Chemistry* (p. 621).
9. C, C. (1991). *Overview of technical, engineering and advanced ceramics*. In: *Engineered Materials Handbook, Ceramic and Glasses. Vol. 4*. ASM International.
10. CBE, R. S. (1999). Ceramics and glasses. In *Modern Physical Metallurgy and Materials Engineering (Sixth Edition)* (pp. 320-350).
11. CivanPhD, F. (2016). Instrumental and Laboratory Techniques for Characterization of Reservoir Rock. In *Reservoir Formation Damage (Third Edition)*.
12. Clarke, D. R. (1989). Issues in the Processing of Cuprate Ceramic Superconductors. *Journal of the American Ceramic Society*, 72(7), 1103-1113.
13. Coble, R. (1997). Effect of magnesia on the densification behavior and grain growth of nucleated gel alumina. *Materials Chemistry and Physics*, 47(1), 78-84.
14. Cutler, I. B. (1957). Sintering of Alumina at Temperatures of 1400°C. and Below. *J. Am. Ceram. Soc*, 4, 134-139.
15. D.Hayes, M. (2015). *Fractography as a Failure Analysis Tool*. Plastics Design Library.
16. D.Hayes, M. (2015). Fractography in Failure Analysis of Polymers. *Plastics Design Library*, 1-5.
17. Erkalfa, H. (1996). Effect of additives on the densification and microstructural development of low-grade alumina powders. *Journal of Materials Processing Technology*, 62, 108-115.

18. Fahrenholtz, W. G. (2004). *Ceramic Engineering III Sintering*.
19. Faoite, D. d. (2012). A review of the processing, composition, and temperature-dependent mechanical and thermal properties of dielectric technical ceramics. *Journal of Materials Science*, 47, 4211-4235.
20. FatimaZivic. (2021). *General Overview and Applications of Ceramic Matrix Composites (CMCs)*. Science Direct.
21. Fu, Y. (2016). The role of CuO–TiO₂ additives in the preparation of high-strength porous alumina scaffolds using directional freeze casting. *Journal of Porous Materials*, 23, 539-547.
22. GERMAN, R. M. (1996). Solid-State Sintering Fundamentals. In *Sintering Theory and Practice*.
23. Ghorbal, G. B. (2017). Comparison of conventional Knoop and Vickers hardness of ceramic materials. *Journal of the European Ceramic Society*, 37(6), 2531-2535.
24. HaiyangLi. (2017). Low-temperature sintering of coarse alumina powder compact with sufficient mechanical strength. *Ceramics International*, 43(6), 5108-5114.
25. HaiyangLi. (2017). Low-temperature sintering of coarse alumina powder compact with sufficient mechanical strength. *Ceramics International*, 43(6), 5108-5114.
26. Haldar, P. (2020). Effect of Nano CuO Addition on the Tribo-Mechanical Behavior of Alumina Ceramics in. *International Journal of Applied Ceramic Technology*, 18(1), 110-118.
27. Haldar, P. (2020). Effect of nano CuO addition on the tribo-mechanical behavior of alumina ceramics in non-conformal contact. *International Journal of Applied Ceramic Technology*, 18(1), 110-118.
28. Heimann, R. B. (2010). *Classic and Advanced Ceramics: From Fundamentals to Applications*. Wiley-VCH.
29. Hori. (1990, January 9). *Us Patent No. 4,892,850*.
30. Hossen, M. (2014). Effect of Zirconia Substitution on Structural and Mechanical Properties of ZTA Composites. *Journal of mechanical and civil engineering*, 2(2), 1684.
31. Hossen, M. M. (2014). Effect of Zirconia Substitution on Structural and Mechanical. *Journal of Mechanical and Civil Engineering*, 11(2), 01-07.
32. Huhtamäki, T. (2018). Surface-wetting characterization using contact-angle measurements. *Nature Protocols*, 12, 1521-1538.
33. J.Svoboda. (1996). A model for liquid phase sintering. *Acta Materialia*, 44(8), 3215-3226.
34. Kingery, W. (1976). *Introduction to Ceramics*.

35. Kingery, W. D. (1959). Densification during Sintering in the Presence of a Liquid Phase. I. Theory. *Journal of Applied Physics*, 30, 301.
36. KUMARI, S. (2013). *Effect of TiO₂ Addition in Al₂O₃: Phase Evolution, Densification, Microstructure And Mechanical Properties*.
37. L.L, H. (1988). *Ceramics and the challenge of change* . Ad.Ceram.Mater.
38. Lowell, S. (2004). Density Measurement. In *Characterization of Porous Solids and Powders: Surface Area, Pore Size and Density*.
39. Medvedovski, E. (2006). Alumina–mullite ceramics for structural applications. *Ceramics International*, 32, 369-375.
40. Montedoa, O. R. (2018). Effect of LZSA Glass–Ceramic Addition on Pressureless Sintered Alumina. *Materials Research.*, 21.
41. Mordfin, L. (1968). Strength Testing Of Ceramics—A Survey. *Symposium held at Gaithersburg, Maryland*, 243.
42. Möser, M. (1978). FRACTOGRAPHIC ANALYSIS OF FAILURES. *7th Congr. Materials Testing, Budapest*, 2, 851-855.
43. Odaka, A. (2008). Densification of Ca-doped alumina nanopowders prepared by a new sol–gel route with seeding. *Journal of the European Ceramic Society*, 28, 2479-2485.
44. Pelleg, J. (2014). *Mechanical Properties of Ceramics*. Springer Cham.
45. Petzow, G. (1984). Basic Mechanisms of Liquid Phase Sintering. In *Sintering Key Papers* (pp. 51-70).
46. Prakash, R. (n.d.). Optical and x-ray photoelectron spectroscopy of alpha alumina. *AIP Conference*.
47. Quesada, D. E. (2019). Introductory Chapter: Ceramic Materials - Synthesis, Characterization, Applications and Recycling. In *Ceramic Materials - Synthesis, Characterization, Applications and Recycling*.
48. Radonjić, L. (1997). Effect of magnesia on the densification behavior and grain growth of nucleated gel alumina. *Materials Chemistry and Physics*, 47, 78-84.
49. RainerTelle. (2014). *Properties of Ceramics, Handbook of Ceramics Grinding and Polishing*.
50. Randall M. German. (2009). Review: liquid phase sintering. *Journal of Materials Science volume* , 44, 1-39.
51. SadatMirdamadi, E. (2021). *Metal oxide-based ceramics*. Science Direct.

52. Seiler, H. (1983). Secondary electron emission in the scanning electron microscope. *Journal of Applied Physics*, 54.
53. SerkanAball. (2011). Effect of TiO₂ doping on microstructural properties of Al₂O₃-based single crystal Ceramics. *Journal of Ceramic Processing Research*, 12(1), 21-25.
54. Silvestre, J. (2015). An overview on the improvement of mechanical properties of ceramics nanocomposites. *Journal of Nanomaterials*, 2015, 3.
55. Sines, G. R. (2013). *Compression Testing of Ceramics*. Springer New York, NY.
56. Sing, R. (2008). Effect of Copper Oxide on the Sintering of Alumina Ceramics. *Advanced Materials Research*, 47-50, 801-804.
57. Subedi, M. M. (2013). Ceramics and its Importance. *The Himalayan Physics*, Vol.4, No.4, July, Vol. 4.
58. Swab, J. J. (2019). Dynamic Compression Strength of Ceramics: Results from an Interlaboratory Round-Robin Exercise . *ASTM International* . , 58.
59. Swab, J. J. (2021). Dynamic Compression Strength of Ceramics: What was Learned from an Interlaboratory Round Robin Exercise. *Journal of Dynamic Behavior of Materials*, 7, 34-47.
60. Ullner, C. (2001). Hardness testing on advanced technical ceramics. *Journal of the European Ceramic Society*, 21(4), 439-451.
61. Voytovych, R. (2002). The effect of yttrium on densification and grain growth in α -alumina. *Acta Materialia*, 50, 3453-3463.
62. Xu, L. (2015). Sintering and Performance of High Alumina Refractory with ZrO₂ Addition. *Characterization of Minerals, Metals, and Materials* , 503-507.